BDX-613-1723 (Revised)

MACHINABILITY OF METALS AS RELATED TO MINIATURE PRECISION COMPONENTS

Topical Report

L. K. Gillespie, Project Leader

Project Team:
R. K. Albright
B. J. Neal

Published January 1978

Prepared for the United States Department of Energy
Under Contract Number EY-76-C-04-0613.

Bendix Kansas City Division

DISCLAIMER

Printed in the United States of America

Available From the National Technical Information Service, U.S. Department of Commerce, 5285 Port Royal Road, Springfield, Virginia 22161.

Price: Microfiche $3.00
Paper Copy $6.50

BDX-613-1723
Distribution Category UC-25

MACHINABILITY OF METALS AS RELATED TO MINIATURE PRECISION COMPONENTS

BDX-613-1723

Published January 1978

Project Leader:
L. K. Gillespie
Department 822

Project Team:
R. K. Albright
B. J. Neal

Topical Report

Communications Services

Bendix Kansas City Division

MACHINABILITY OF METALS AS RELATED TO MINIATURE PRECISION COMPONENTS

BDX-613-1723, UNCLASSIFIED Topical Report, Published January 1978

Prepared by L. K. Gillespie, D/822.

A study to determine how tool geometry and workpiece material can be selected to produce low cutting forces, small fillet radii, smooth surface finishes, and burr-free edges required for the production of reliable miniature precision parts has indicated that tool geometries typically specified for general machining applications produce optimum results. Surface finishes of 0.56 to 1.07 μm AA (22 to 40 microinches) can be produced while maintaining 76.2-μm (0.003 inch) fillet radii in ferrous and beryllium-copper alloys. Tool life is extremely short when fillet radii less than 76.2 μm must be maintained. Materials having high strain-hardening exponents produce large burrs.

WPC-bap

The Bendix Corporation
Kansas City Division
P. O. Box 1159
Kansas City, Missouri 64141

A prime contractor with the United States Department of Energy under Contract Number EY-76-C-04-0613

THIS PAGE
WAS INTENTIONALLY
LEFT BLANK

CONTENTS

THIS PAGE
WAS INTENTIONALLY
LEFT BLANK

ILLUSTRATIONS

TABLES

SUMMARY

Component parts of small mechanisms often require surface finishes of 0.406 to 0.812 μm (16 to 32 microinches), nearly sharp edges, and very small fillet radii. In addition, edges generally must be free of burrs to assure reliable operation of the mechanism.

Because of the importance of knowing before machining is begun how workpiece material and tool geometry will affect such variables as surface finish, fillet radius, burr size, and cutting forces, this study was directed toward determining the machinability of materials that commonly are used in the production of miniature precision components. Optimum machinability was defined in terms of the variables studied.

A second goal of the study was to develop equations which would predict optimum tool geometries from a knowledge of workpiece properties.

For the evaluation of five tool-geometry variables, more than 4000 measurements were made on more than 500 test samples from six different materials. In addition, the influence of the depth-of-cut and the number of specimens machined also was studied.

Surface finishes of 0.56 to 1.07 μm AA (22 to 42 microinches) can be produced while maintaining 76.2-μm (0.003 inch) fillet radii. Tool life is extremely short when maximum fillet radii of 50.8 μm (0.002 inch) are required. Burr height and burr thickness were found to increase as the strain-hardening exponent of the workpiece becomes greater. Low feedrates were found to increase the unit cutting power up to three times that which normally is experienced.

Optimum tool geometries that were observed in this study proved to be similar to those that are recommended in machining handbooks for general use.

DISCUSSION

SCOPE AND PURPOSE

This study was initiated with the following three objectives:

- To determine which materials that are common to parts produced at Bendix Kansas City are easily machinable, where machinability is based on miniature-precision-part criteria;
- To develop equations which will relate machinability and tool design to the properties of the materials; and
- Insofar as possible, to rank the materials by dimensional stability.

The described tests were made to provide quantitative comparisons of machinability and to develop equations for predicting optimum cutting-tool geometry from a knowledge of workpiece properties.

PRIOR WORK

A previous report has been prepared on this subject,[1] and a related study of carbide cutting-tool materials also has been reported. The latter study, however, is not directly applicable to miniature parts because of the large tool-nose radii used.

ACTIVITY

In the production of miniature precision mechanisms, the machinability of the workpiece material determines the sequence of manufacturing operations, the machining time, and the tool design. Although machinability ratings have been established for "roughing" conditions, neither quantitative nor qualitative ratings have been established for the conditions required for machining miniature precision parts. In many instances, a material different from that originally conceived is used for components in order to minimize fabrication costs. In making such substitutions, a knowledge of the significance of the changes is of extreme importance.

Whenever new materials are specified for precision parts, manufacturing plants spend a considerable amount of time in developing optimum cutting-tool geometries. A trial-and-error approach to the development of tool geometry can noticeably increase the lead time required to manufacture the first group of parts. The development of equations to predict optimum tool geometry from a knowledge

of workpiece mechanical properties would minimize much of this initial experimentation.

While machinability has been defined many different ways,[3,4] the following equation usually is used for comparing the machinability of different materials.

$$I = 100\left(\frac{V_{t20} \text{ of the material being tested}}{V_{t20} \text{ of the standard material}}\right), \quad (1)$$

where

I = the machinability rating or index, and

V_{t20} = the cutting velocity which provides a 20-minute tool life.

AISI B1112 is the standard reference material that is used most often. In most cases, tool life is defined as the cutting time required to produce a wearland of a given size on the tool. Different wearland end-points are chosen for different cutting-tool materials and different types of operations.[5]

While definitions of machinability such as these are good relative measures for general machining operations, they are constructed for a fixed set of machining conditions (tool-nose radius, depth-of-cut, feedrate, etc). For use over a wide range of conditions, however, data must be obtained for a number of different combinations. This is one reason why extensive tables of recommendations such as those found in the *Machining Data Handbook*[6] are more useful to the manufacturing engineer than a single rating. In using any of these approaches, however, the fact should be realized that the data published to date pertain to reasonably large stock. The conditions shown in Table 1, for example, approximate the conditions that are used most often to produce the indicated results. Typical requirements for turned miniature precision parts are shown in Table 2.

Requirements such as the 76.2-μm (0.003 inch) maximum fillet radius necessitate the use of turning tools having nose radii of 76.2 μm, or smaller. Achieving the indicated surface finish with such a sharp-nosed tool requires slowing feedrates to less than 12.7 μm/revolution (0.0005 ipr). The close dimensional tolerance necessitates frequent tool adjustment and the maintenance of low cutting forces (since large forces will bend small shafts and cause taper). Burr size must be minimized in order to utilize deburring processes that will not adversely affect dimensions while removing the burrs. Most processes will remove burrs that are thinner than 25.4 μm (0.001 inch) without removing more than 5.08 μm (0.0002 inch) from a diameter or exceeding an edge break

Table 1. Conditions Typically Used to Generate Machinability Data for Lathe Operations

Machining Condition	Value
Feedrate	76.2 to 254 μm/revolution (0.003 to 0.010 ipr)
Nose Radius	0.76 mm (0.030 inch)
Depth-Of-Cut	0.38 to 1.25 mm (0.015 to 0.050 inch)

Table 2. Typical Requirements for Turned Miniature Precision Parts

Requirement	Value
Surface Finish	0.20 to 0.41 μm (8 to 16 microinches)
Tolerances	±5.08 μm (±0.0002 inch)
Maximum Fillet Radii	76.2 μm (0.003 inch)
Minimum Burr Size	25.4 μm (0.001 inch) or less
Maximum Edge Breaks	76.2 μm (0.003 inch)

of 76.2 μm (0.003 inch). This is particularly important for extremely small pins. For example, pins having a diameter of 0.5 mm (0.020 inch) are very difficult to deburr without excessive stock losses when the burrs to be removed range up to 76.2 μm in thickness.

Figure 1 illustrates the need for maintaining a small fillet radius on a typical miniature part. As shown, thin working parts must have nearly sharp edges to provide sufficient bearing area. A 0.5-mm-wide (0.020 inch) pawl having a 127-μm (0.005 inch) edge radius on both sides would result in a contact-surface width of only 254 μm (0.010 inch) with the mating part; a 50.8-μm (0.002 inch) radius on each side of the pawl would provide a 60-percent increase in the bearing surface.

The fillet radius on a part must be smaller than the edge radius on the mating part to assure a flush fit. With laser-welded or electron-beam-welded joints, large radii reduce the amount of metal that is available to fill the weld joint.

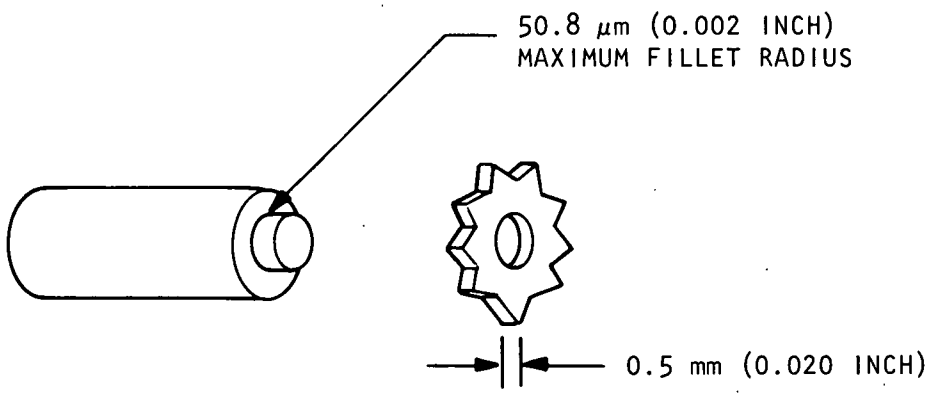

Figure 1. Illustration Showing the Need for Maintaining a Small Fillet Radius to Provide a Precision Fit of Mating Parts

The need for 90-degree shoulders, when combined with the need for tools having small nose radii, necessitates the use of negative side-cutting edge angles (SCEA) in order to both turn and face the part. (A negative side-cutting edge angle indicates that the point of the tool leads the cutting edge; although there is no industry standard for describing this angle under these conditions, the use of a negative sign is compatible with the designation used for rake angles.) The negative SCEA results in a very weak tool nose (Figure 2) which may be easily chipped and quickly worn away. These conditions, in turn, greatly affect the part dimensions.

From the examples given, the inadequacy of conventional approaches for assessing the machinability of the types of parts described can be readily seen. Because of piece-part requirements, defining tool life as the total amount of cutting time accumulated before the occurrence of a given crater wear is no longer sufficient. (Test results indicate that crater wear cannot be correlated to any of the piece-part requirements shown in Table 2.) From a production standpoint, the end of tool life is the point at which any *one* of the first four items listed in Table 2 exceeds the required tolerance value shown.

Unfortunately, in any test, machinability is also a function of the tool geometry used. Thus in order for the test results to be meaningful, they must be based on the tool geometry that typically is used, or on the optimum geometry. Because this factor varies with different workpiece materials, another variable must be included in the machinability results.

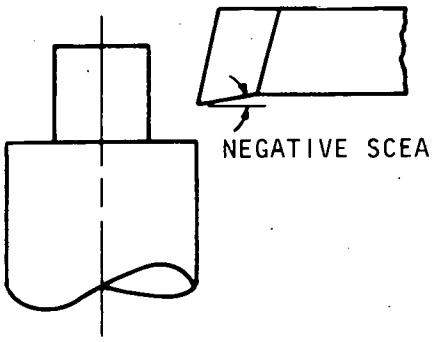

CONVENTIONAL TURNING TOOL

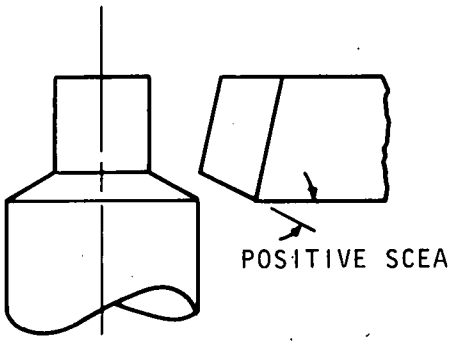

FACE-AND-TURN TOOL

Figure 2. Comparison Between Conventional Turning Tool and Face-And-Turn Tool

Test Approaches

Two distinct tests were performed during this study. In the first test, the change in the fillet radius was monitored as a function of the length of material cut. These results were compared with results that had been previously reported. In the second test, 13 dependent variables were recorded for turning cuts in 6 materials using 16 tool-geometry and depth-of-cut combinations. An analysis of variance was performed to determine which cutting parameters influenced each of the dependent variables. The effectiveness of each condition was ranked by variable, and the typically best geometries were noted.

Regression analyses then were performed to relate independent and dependent variables. Equations for predicting optimum tool geometries as functions of workpiece properties were generated by regression analysis. Optimum conditions were defined as minimum burr, minimum wear, minimum forces, etc.

Fillet-Radius Test

In the test of fillet radius produced by sharp tools, a 12.7-mm-long by 127-μm-wide (0.5- by 0.005-inch) cut was made on 87 specimens. The material consisted of 3.175-mm-diameter (0.125-inch) 17-4PH stainless steel in the H900 condition. The material was machined at a speed of 1100 rpm (187.96 mm/s or 37 sfpm) and a feedrate of 0.425 mm/s (1.625 ipm). The metal-removal rate for these conditions was 273 mm^3/s (0.003 $in.^3/min$).

The tool geometry consisted of a 5-degree back rake (BR) and end relief (ERf), a 10-degree side rake (SR), a 7-degree end-cutting edge angle (ECEA) and side relief (SRf), and a -2-degree side-cutting edge angle (SCEA). The tool was ground from cobalt high-speed steel (HSS) (manufactured by the Cleveland Twist Drill Company, List No. 855 Mo-Max). A sulfur-base coolant was brushed on during the cut, and two tools were used to provide a measure of repeatability. Fillet radii were measured by the use of an optical comparator.

The results of these tests (Figures 3, 4 and 5) indicate that tool life is from approximately 508 to 635 mm (20 to 25 inches) of cut under the conditions described. These figures roughly represent 25 to 50 piece parts. Although the fillet radius did not exceed 50.8 μm (0.0020 inch) for the conditions studied, the trend indicates that some additional wear can be expected with little additional cutting.

In most production situations, a tool life which corresponds to a 60-minute cutting-time is considered desirable for HSS tools. In this test, the effective life was only one-fourth of that amount. In addition to necessitating the use of low feedrates, the 50.8-μm (0.002 inch) maximum-fillet-radii requirement obviously increases the tool-change frequency and thus further decreases productivity.

Previously reported results using C7-solid-carbide inserts, a 0-degree BR, a 6-degree SR, a 5-degree ERf and ECEA, and a -8-degree SCEA are similar in their order of magnitude.[7] Fillet radii increased to 50.8 μm (0.002 inch) after only 254 mm (10 inches) of cut when 12.7-mm-diameter (0.5 inch) specimens were cut at a speed of 925 rpm and a feedrate of 2.98 mm/s (0.007 ipr). The fact should be noted that, under the latter conditions, fillet radii of 50.8 μm (0.002 inch) were maintained at this high feedrate for up to 2.54 m (100 inches) of cut.

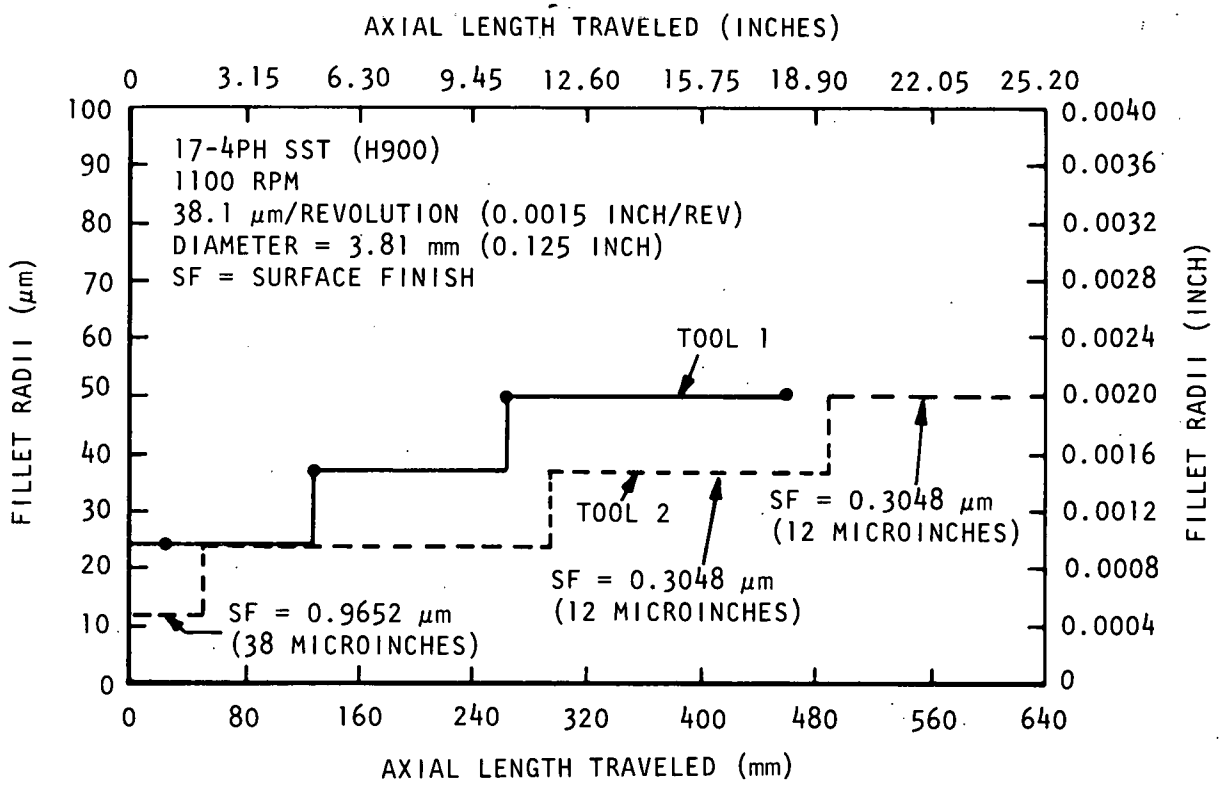

Figure 3. Axial Length Traveled Versus Fillet Radii Produced

Tests of Tool-Geometry Effects

Test Approach

In this study, six workpiece materials that are common to current Bendix miniature precision parts were studied. Five tool angles were studied, as was the radial depth-of-cut (Table 3). All tests were performed at a constant speed and feedrate on a Hardinge HLV lathe. The properties that were measured included three orthogonal cutting forces (Figure 6) together with the workpiece fillet radius, surface finish, burr height, and burr thickness. Tool properties that were measured included the wearland thickness at three points, the radial wear, and the nose-radius wear.

Test specimens were centerless-ground to a diameter of 24.89 mm (0.980 inch) to remove contaminating materials in the skin. Two specimens, each 28.58 mm (1.125 inches) long were turned with each tool. After turning to the 28.58-mm length, the tool was returned to the beginning of the cut, reset to give the desired depth-of-cut, and fed for 25.4 mm (1.0 inch). This was repeated

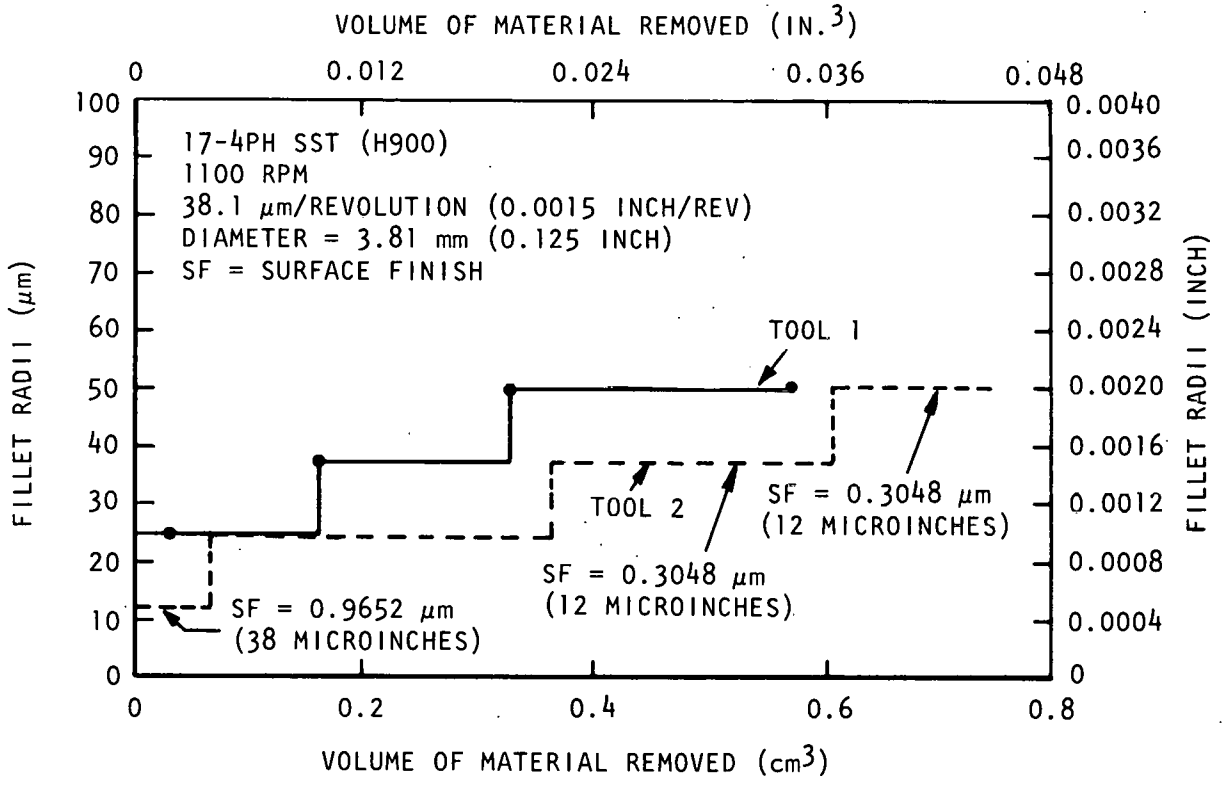

Figure 4. Volume of Material Removed Versus Fillet Radii

for a total of nine passes, with each pass being 3.18 mm (0.125 inch) shorter than the previous one (Figure 7). This technique provided 142.875 mm (5.625 inches) of cut in a specimen only 28.575 mm (1.125 inches) long. A water-soluble coolant was used on all cuts.

A three-axis dynamometer utilizing ceramic strain gages was used to measure the cutting forces. Although capable of measuring forces up to 4.448 kN (1000 pounds), this dynamometer has a sensitivity of 4.448 N (1 pound), or less.

The workpiece materials that were studied included 303Se, 15-5PH and 18-2 stainless steels, Kovar, beryllium copper, and Hiperco 50. The 18-2 stainless steel has been recently developed. It is advertised as having twice the machinability of 303 stainless steel with equivalent mechanical properties and resistance to corrosion. Kovar is a very ductile glass-sealing alloy, and Hiperco 50 normally is a very brittle magnetic material having low hysteresis. Workpiece properties, as measured from in-house tensile specimens, are shown in Table A-1 of the Appendix.

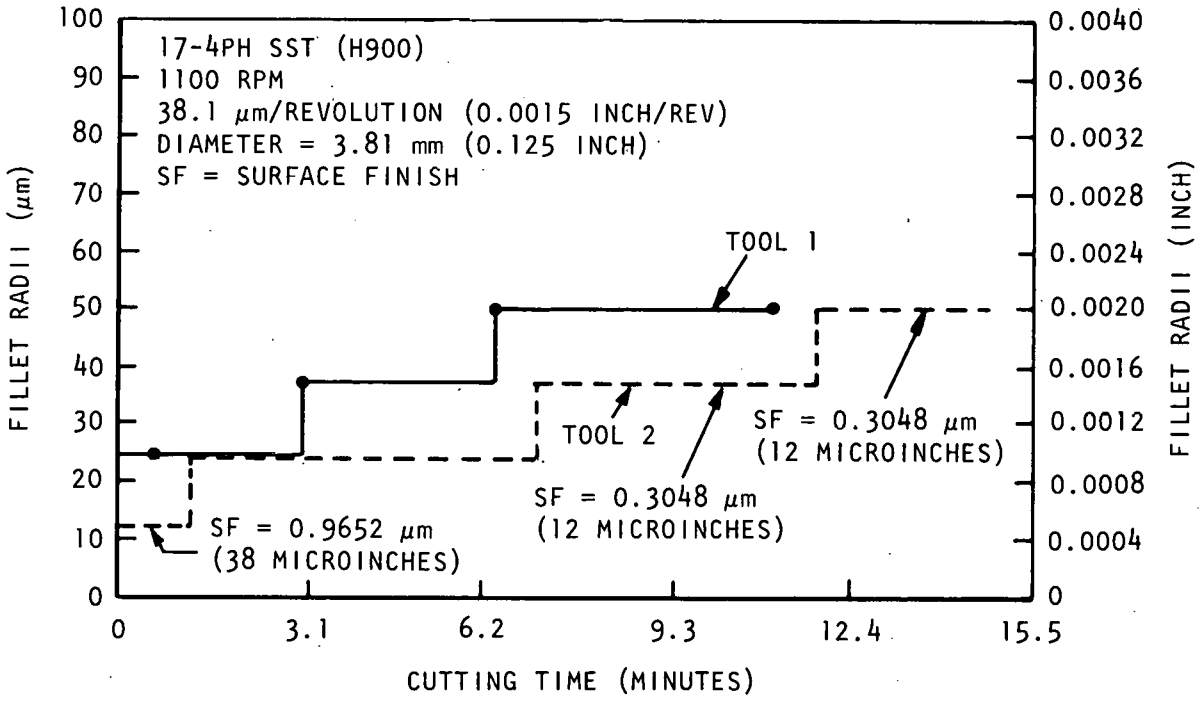

Figure 5. Cutting Time Versus Fillet Radii

The feedrate used in this test was 36.6 μm/revolution (0.00144 ipr), and the spindle speed was 300 rpm. The tool material consisted of List No. 855 Mo-Max Cobalt HSS, manufactured by the Cleveland Twist Drill Company. Ten specimens were produced for each of eight tool geometries in five materials. This one-eighth fractional factorial experiment has been previously described.[1] The averages for the data obtained from the present study are presented in Tables A-2 through A-13 of the Appendix.

The factor codes in the Appendix tables correspond to the factors and levels shown in Table 3. For example, a code of 121212 indicates that Factor A is at Level 1, B is at Level 2, C is at Level 1, etc. Thus the tool would have an ECEA of 7 degrees, an end relief of 5 degrees, a back rake of 5 degrees, a side rake of 5 degrees, an SCEA of -8 degrees, and a depth-of-cut of 127 μm (0.005 inch).

Statistical Considerations

To completely evaluate two levels each of five cutting-tool angles, two depths-of-cut, and six workpiece materials would require 384 separate cutting-combinations. Therefore, to minimize the number of tests required, a fractional factorial experimental

Table 3. Levels of Factors Used in Experiment

Variable and Symbol	Level 1*	Level 2	Level 3	Level 4	Level 5	Level 6
A End-Cutting Edge Angle (ECEA)	7.0	2.0				
B End Relief (ERf)	10.0	5.0				
C Back Rake (BR)	5.0	0.0				
D Side Rake (SR)	10.0	5.0				
E Side-Cutting Edge Angle (SCEA)	-8.0	-2.0				
F Depth-Of-Cut	635** (0.025)	127 (0.005)				
Material	303Se	15-5PH	BeCu	Kovar	Hiperco	18-2

*All "Level" values are in degrees unless otherwise noted.
**Basic "Depth-Of-Cut" values are in micrometers; parenthetical values are in inches.

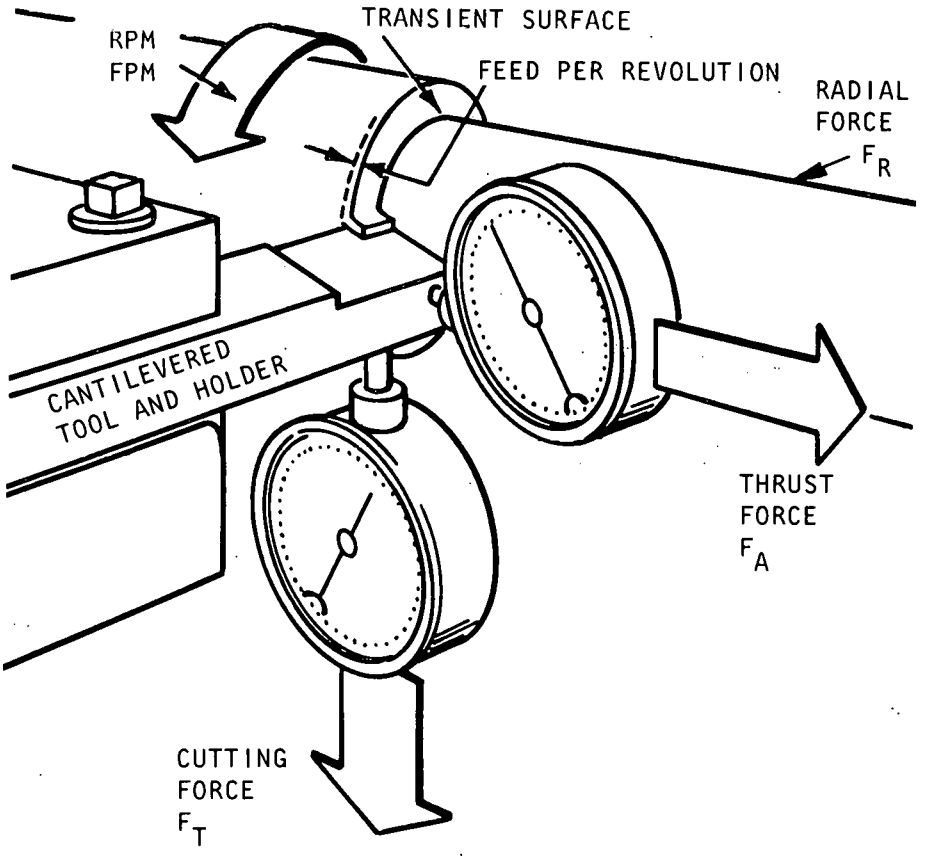

Figure 6. Forces on Cutting Tool During Turning

design was utilized in which only 16 tools were used in each of the six materials. While this one-fourth test replica requires that several assumptions be made, it allows usable results to be obtained with relatively little expense.

In analyzing this type of data, the analyst must decide whether an observed effect is the result of a specific variable or the result of two or three variables acting simultaneously. The height of the three peaks in Figure 8, for example, cannot be predicted by a knowledge of the average slope in the XZ plane and the average slope in the YZ plane; the height is a unique combination of X and Y. In Figure 9, however, the Z location of any point in the top plane can be predicted from the average properties in the YZ and XZ planes. In this case, there is no interaction of variables to produce unusual changes in the Z direction; any change in Z is strictly a function of the main effects of Variables X and Y.

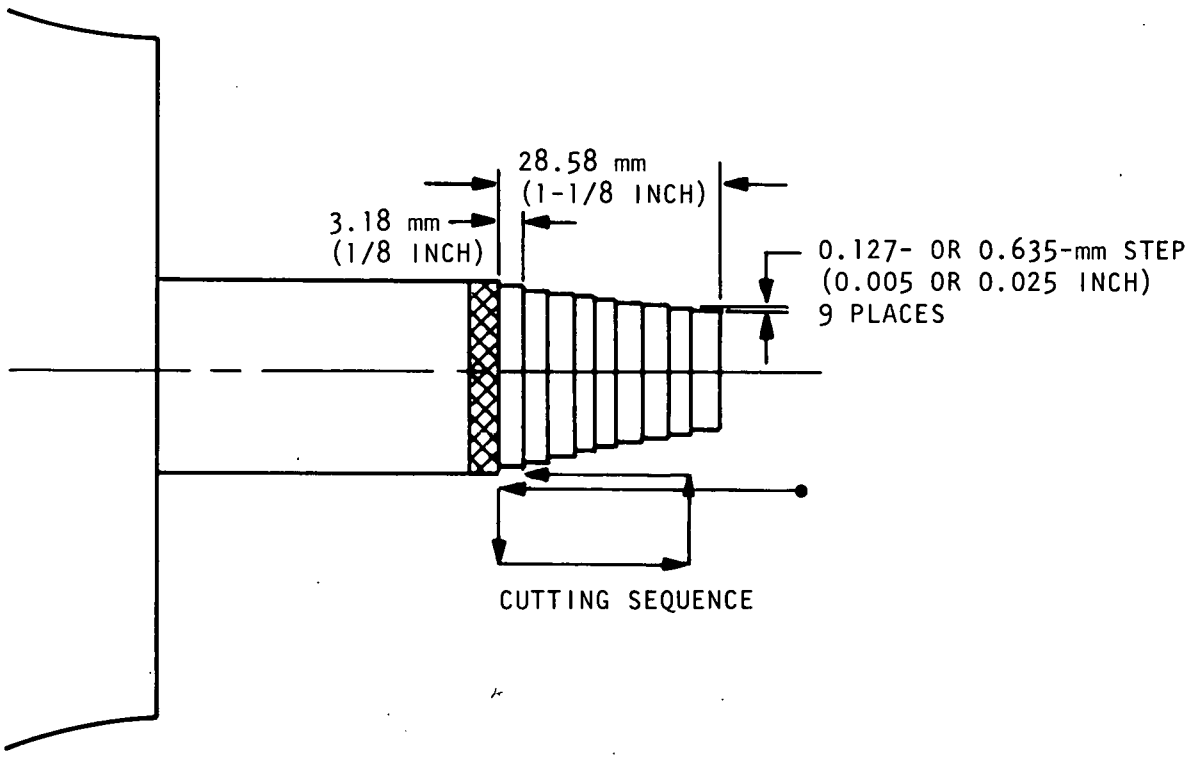

Figure 7. Configuration and Cutting Sequence of Test Specimens

If the 384 distinct cutting conditions were completely tested, a determination of whether some specific combination of variables produced a unique result could be easily made. With 192 conditions, a determination could be made of whether two, three, or up to six variables had acted together to produce a unique perturbation. With only 16 conditions, a determination can be made of whether some combination of two variables produces a significant effect, and whether single variables (such as depth-of-cut or back rake) have influenced the results. This latter procedure generally is adequate, since higher-order interactions seldom exist or seldom are meaningful in industry. All of the following comments in this report are based upon the validity of this assumption.

Test Results of Tool-Geometry Effects

Specific Geometry Effects

An analysis of variance (ANOVA) was performed on the raw data. The results obtained are shown in Tables A-14 through A-20 of the

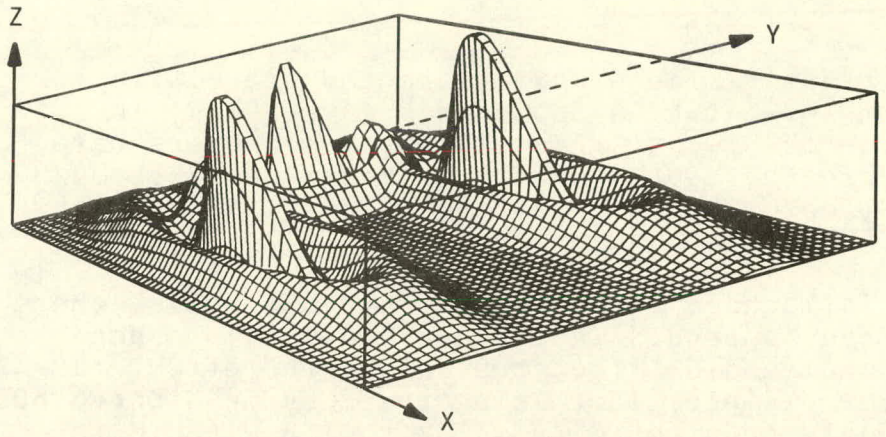

Figure 8. Graphic Illustration of Two-Factor Interactions Between Variables X and Y Which Produce Significant Differences in Response Variable Z

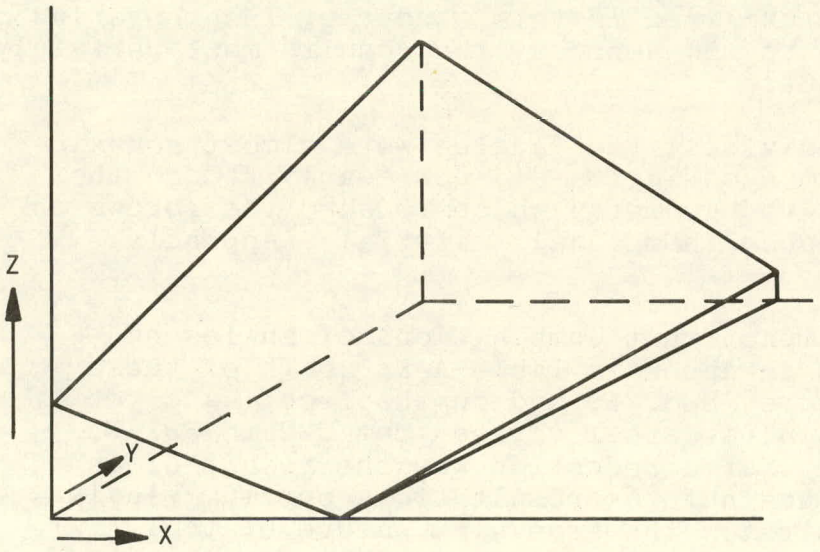

Figure 9. Illustration of Case in Which Variables X and Y Affect Variable Z Without Any Two-Factor Interactions

Appendix. The alias structure for the analysis is shown in Table A-21. Because of the large number of statistically significant results that were obtained, only those that are particularly significant to production are discussed in this report.

Principal Cutting Force F_T

The single most important variable which affected the cutting force F_T was the depth-of-cut. As shown in Figure 10, F_T is proportional to the depth-of-cut. (Most other researchers have noted this fact for greater depths-of-cut.) Equations 2 through 7, listed in Table 4, describe this cutting force as a function of the depth-of-cut.

While other factors influenced force F_T for some materials, there was no consistent trend (Appendix Tables A-8 and A-14). When changes in the tool angles did affect the force, the effect was relatively small. For example, increasing the ECEA in Hiperco 50 from 2 to 7 degrees only reduced F_T from 163 to 145 N (36.6 to 32.6 pounds). The effect of changing other angles was even less.

The fact that changing the back rake, side rake, and the other angles did not, by themselves, significantly reduce the cutting forces is surprising, since the literature and theory pertaining to metal cutting indicate that they are major contributors to these forces. The only obvious explanation for this discrepancy is the fact that only the small ranges of angles that are actually used in production were utilized in this study; by incorporating angles ranging from -15 to +15 degrees, the results most certainly would have been different.

While the effects of individual tool angles were almost nonexistent, certain combinations of angles did noticeably reduce the forces. Unfortunately, the geometry which reduced the forces on one material did not reduce them on all materials (Appendix Table A-13).

For an example of the impact that combinations of angles had, consider Tools 1 and 16 in Appendix Table A-8: both of these tools experienced the same feedrate and depth-of-cut, and yet the forces in 303Se stainless steel varied from 222 to 391 N (50 to 88 pounds). This force reduction was the result of an optimum tool geometry, and not the result of an optimum single angle. Figure 11 illustrates the irregular nature of tool geometry in affecting force F_T.

As shown in Figure 10, 303Se stainless steel, which often is called "free machining," exhibited the highest cutting forces among all the materials studied. The 18-2 stainless steel, which reportedly is much easier to machine, required a much smaller cutting force. The 15-5PH stainless steel, which had the highest tensile strength of all the materials studied, required roughly half the cutting force of 303Se stainless steel. These results are not directly related to hardness, as one might assume; the 303Se stainless steel, inadvertently obtained in the annealed condition, was the softest material that was machined.

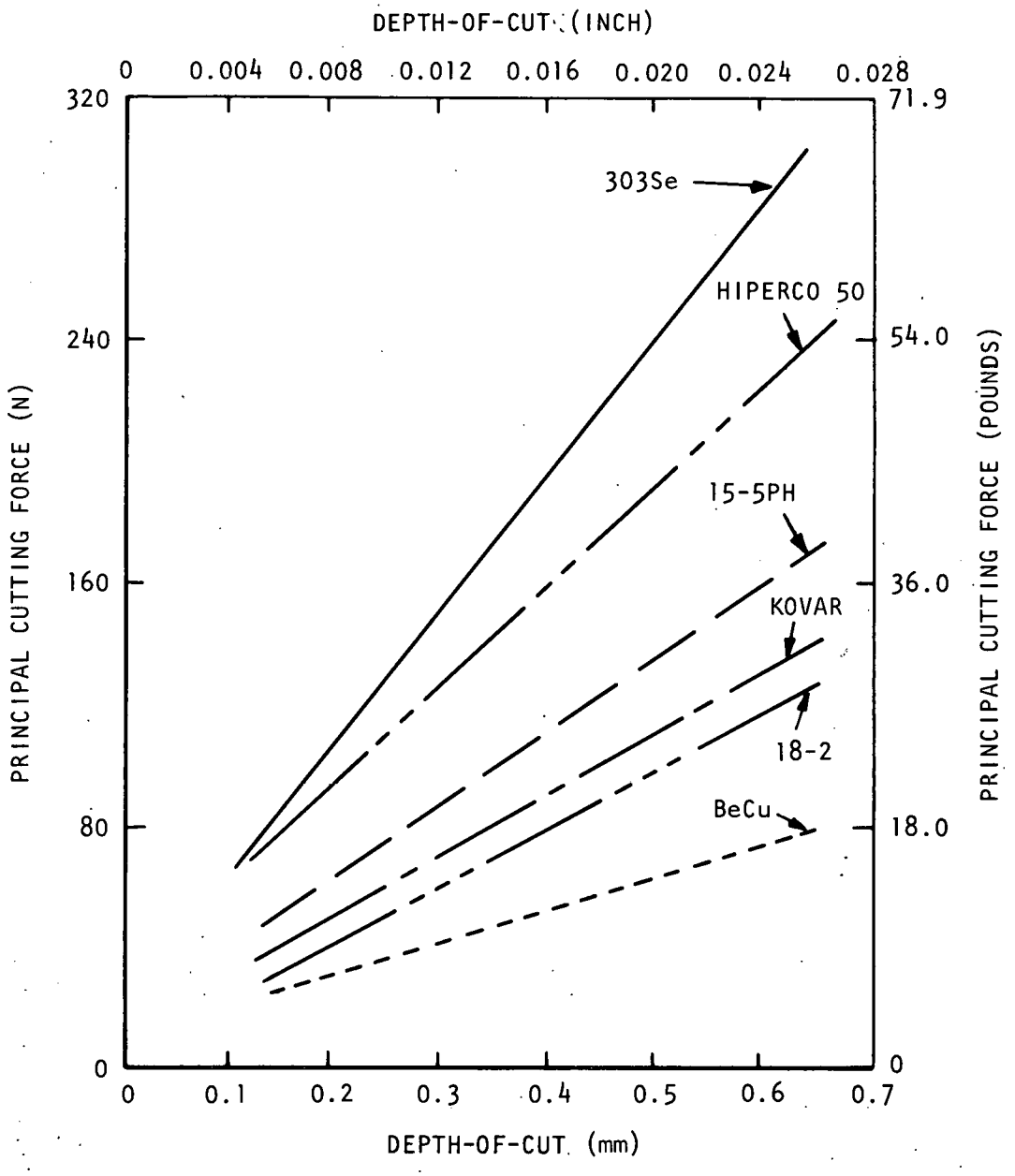

Figure 10. Effect of Depth-Of-Cut on Principal Cutting Force F_T

As previously indicated, large cutting forces tend to cause taper in workpieces, large burrs, and rapid tool wear. Thus they are undesirable for the manufacture of miniature precision components.

Table 4. Equations to Define Cutting Force F_T as a Function of Depth-Of-Cut

Material	Equation*	Equation Designation**
303Se (R_B 91)	$F_T = 4.31 + 2537d$	2
Hiperco 50 (R_C 27)	$F_T = 6.61 + 1866d$	3
15-5PH (R_C 36)	$F_T = 3.36 + 1286d$	4
Kovar (R_B 95)	$F_T = 5.01 + 1054d$	5
18-2 (R_B 99)	$F_T = 0.78 + 1093d$	6
BeCu (R_B 96)	$F_T = 4.25 + 550d$	7

*When F_T is the principal cutting force in pounds, d is the radial depth-of-cut in inches.
**For the purpose of identification in this report only.

As shown in Figure 12, the force F_T is also directly proportional to the feedrate. (The data shown in this figure are for a cold-rolled 303Se stainless steel rather than the annealed material for which all other data were prepared.)

Radial Cutting Force F_R

As shown in Figure 12, Table 5, and Appendix Table A-7, the radial cutting force comprises only about 10 percent of the total value of the principal cutting force F_T. Since it has such a small effect on the workpiece, it, in most analyses, can be ignored.

As in the case of force F_T, increasing the depth-of-cut increased force F_R (Table A-16). In most materials, the end relief angle and the ECEA also affected F_R. A large ECEA reduced force F_R, but a large end relief angle tended to increase F_R.

Axial Cutting Force F_A

The side rake angle and the depth-of-cut significantly affected the axial cutting force F_A (Appendix Table A-15 and Figures 13 and 14). Increasing the depth-of-cut by a factor of 5 increased F_A by a factor of 3 to 5 (Figure 13); increasing the side rake angle by 5 degrees reduced the cutting force F_A by roughly 20 percent.

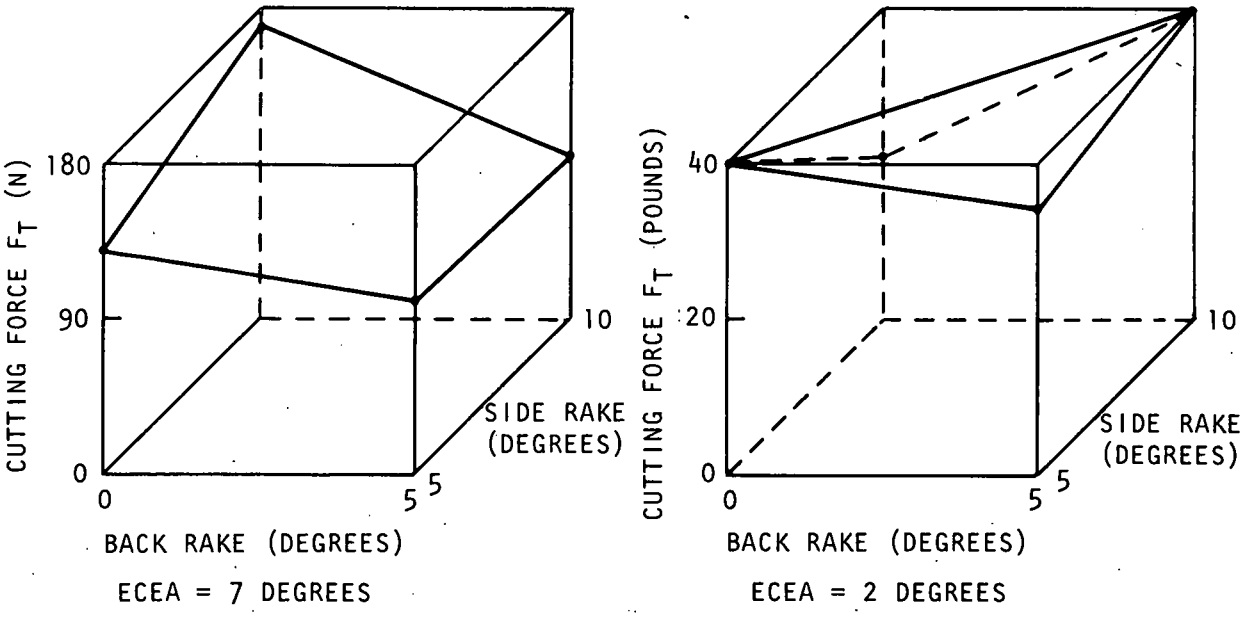

Figure 11. Interactions Between Back Rake and Side Rake for Two Values of ECEA in Hiperco 50

As shown in Table 5, F_A typically is approximately 50 percent of F_T, although this fails to hold true at higher feedrates (Figure 12). Force F_A was affected in Kovar by all of the tool angles studied, and it was affected in 303Se and 18-2 stainless steels by the back rake and the SCEA (Table A-15). In all cases, however, the value of force F_A changed only slightly.

The data shown in Table 5 were obtained by averaging the data shown in Table A-15 of the Appendix over the two levels of variables shown in the coded columns. As in the case of F_T, a large number of interactions were significant; thus some combinations of angles were much better or worse than the averages indicate.

Fillet Radius

Increasing the depth-of-cut increased the fillet radius that was produced on most samples (Figure 15). The reason for this is not obvious, but, for the conditions studied, the increase that was produced in the cutting force by the increased depth-of-cut may have caused greater point wear. For large depths-of-cut where the forces are not concentrated as much at the point as they were in this study, this relationship would not be expected to hold true.

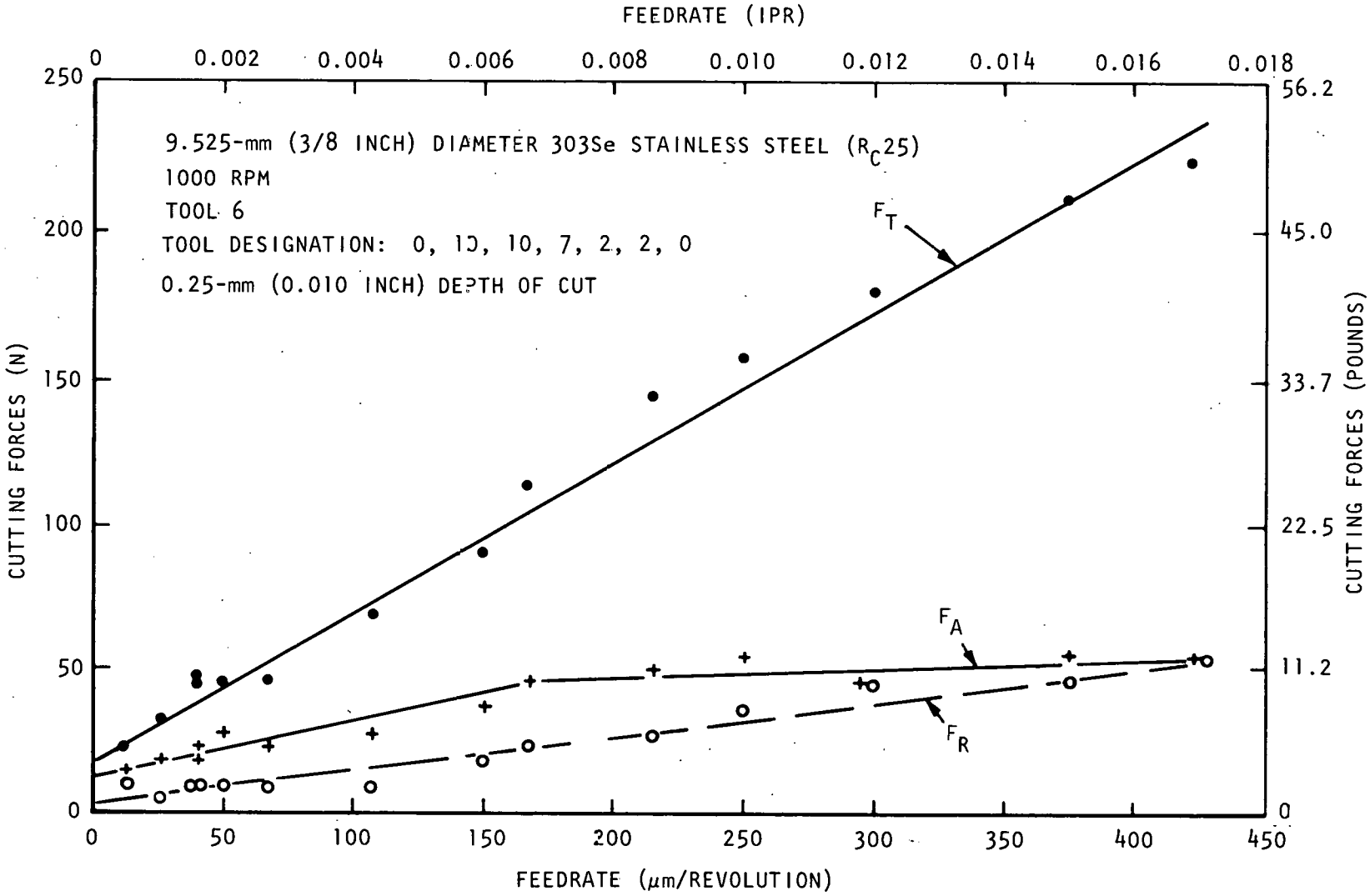

Figure 12. Effect of Feedrate on Cutting Forces in 303Se Stainless Steel

Table 5. Typical Machining Results Produced in Various Materials

Variable Measured	Value Obtained for Material Indicated*					
	303Se	15-5PH	BeCu	Kovar	Hiperco	18-2
Fillet Radii (μm; Inch)	68.6 (0.0027)	58.4 (0.0023)	71.1 (0.0028)	61.1 (0.0024)	99.1 (0.0039)	50.8 (0.0020)
Surface Finish (μm; Microinches)	0.87 (34.4)	0.59 (23.2)	0.89 (35.1)	1.10 (43.5)	0.39 (15.2)	1.27 (50.1)
Burr Height (μm; Inch)	462 (0.0182)	38 (0.0015)	36 (0.0014)	122 (0.0048)	66 (0.0026)	43 (0.0017)
Burr Thickness (μm; Inch)	241 (0.0095)	43 (0.0017)	48 (0.0019)	74 (0.0029)	69 (0.0027)	51 (0.0020)
F_T (N; Pounds)	188.6 (42.4)	107.6 (24.2)	51.6 (11.6)	88.1 (19.8)	153.9 (34.6)	76.5 (17.2)
F_A (N; Pounds)	98.7 (22.2)	47.6 (10.7)	18.7 (4.2)	38.3 (8.6)	62.7 (14.1)	24.9 (5.6)
F_R (N; Pounds)	24.0 (5.4)	3.6 (0.8)	4.9 (1.1)	4.0 (1.0)	12.9 (2.9)	9.3 (2.1)
W_N ($W/cm^3/s$; $HP/in.^3/min$)	4.0 (5.3)	2.4 (3.1)	1.2 (1.6)	1.9 (2.5)	3.6 (4.7)	1.6 (2.1)

*Value shown is the average for 16 tool-geometry/depth-of-cut combinations; each tool produced two specimens each 0.143 m (5.625 inches) long; fillet radius, surface finish, and burr measurements were taken on the final surface and edge produced on each workpiece; one reading was taken on each specimen.

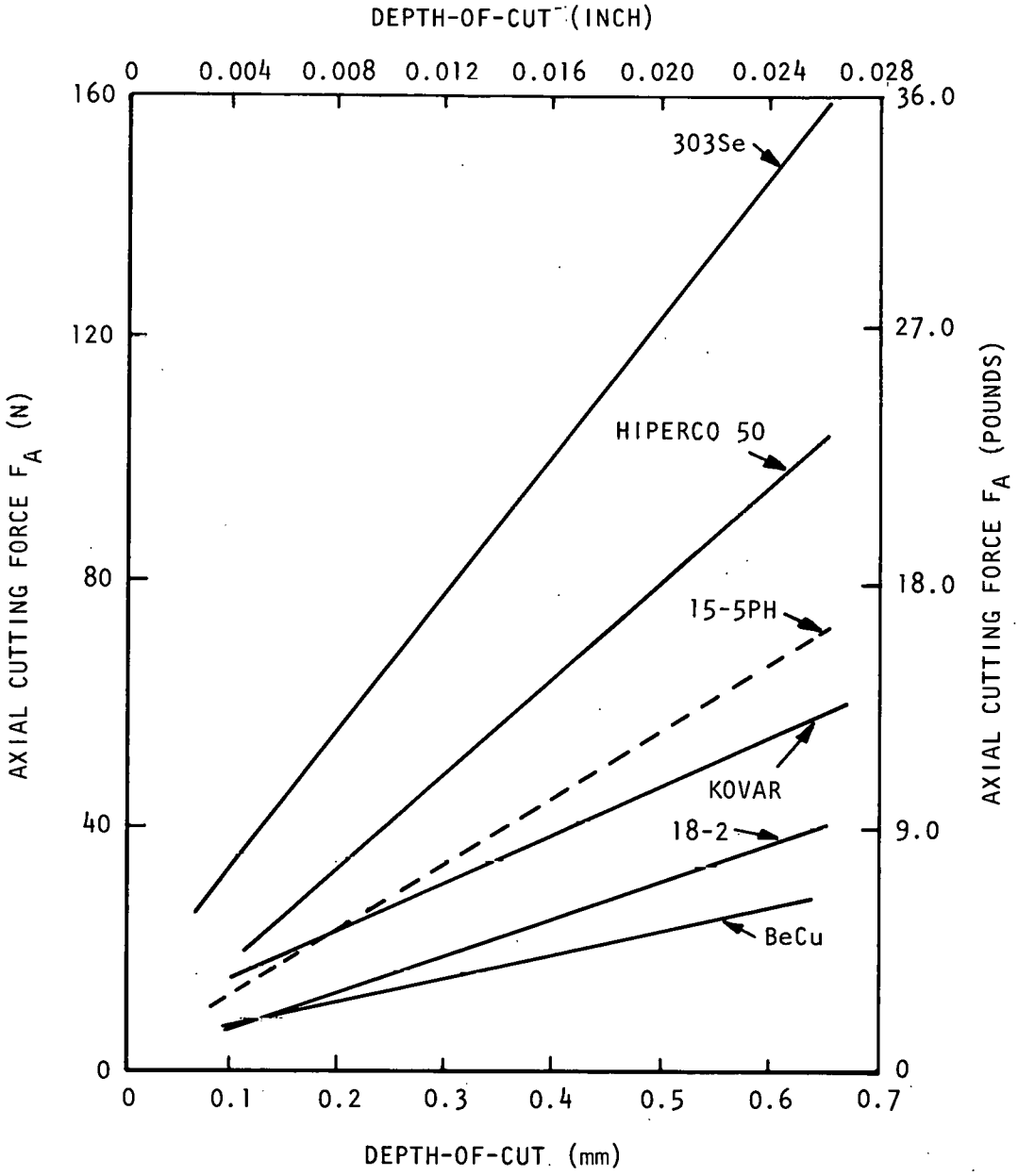

Figure 13. Axial Cutting Force F_A as a Function of the Depth-Of-Cut

Each of the tools had a nose radius of less than 25.4 μm (0.001 inch) when it began the test. The radii shown in the results are the averages of measurements that were taken after 143 mm (5.625 inches) and 286 mm (11.25 inches) of cut; thus they are the radii that would be expected after 213 mm (8.4 inches) of cut.

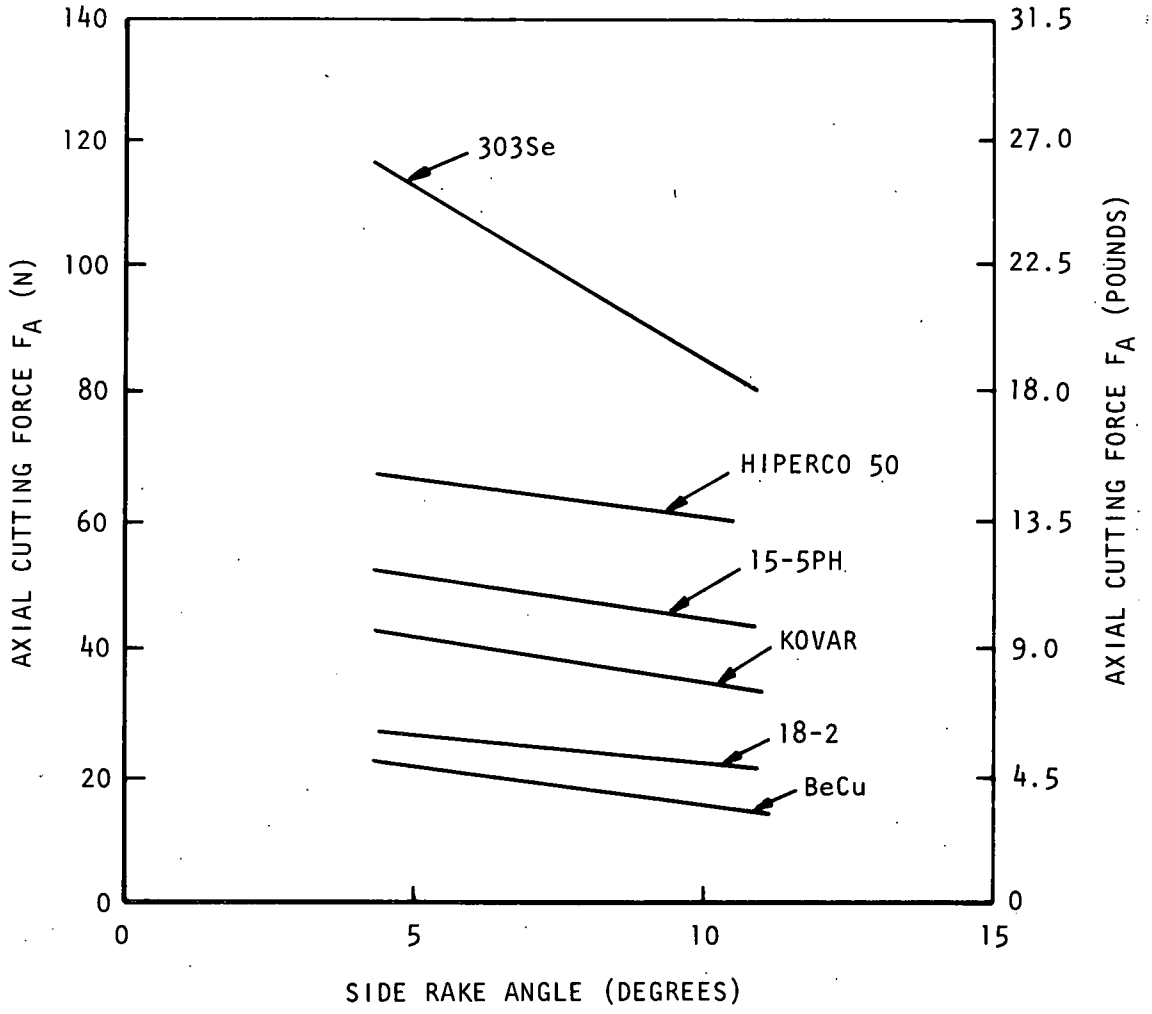

Figure 14. Effect of Side Rake Angle on Axial Cutting Force F_A

Hiperco 50 is a very abrasive material, as evidenced by the large values of wear indicated by the fillet-radii values shown in Figure 15. The significant fact should be noted that the 18-2 stainless steel, advertised to be a more readily machinable equivalent of 303Se stainless steel, experienced less nose-radius breakdown than any of the other materials.

While some tool geometries produced smaller fillet radii than others, there were no identifiable trends (Appendix Tables A-6 and A-17).

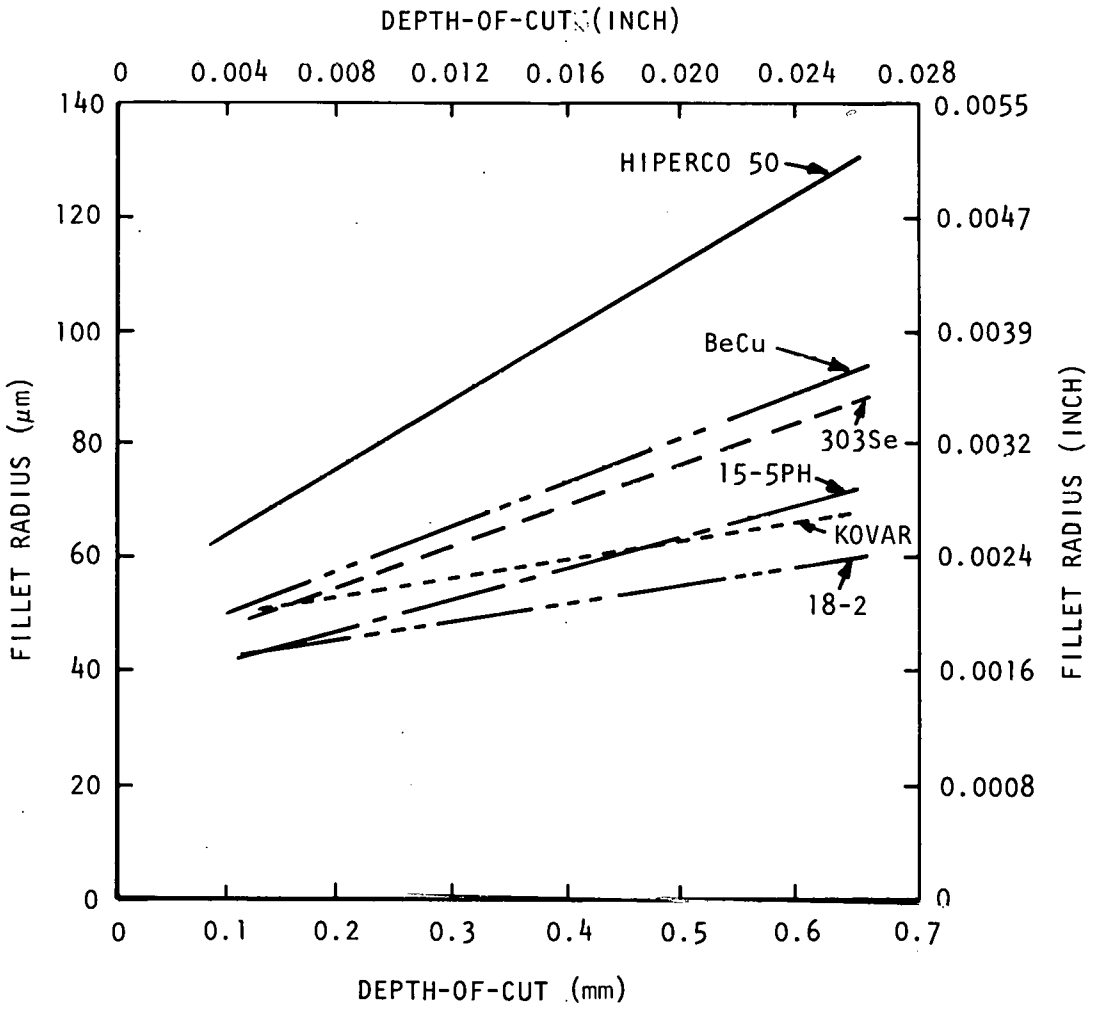

Figure 15. Effect of Depth-Of-Cut on Fillet Radius of Workpiece

Surface Finish

In most of the materials, the ECEA was the only factor that affected the surface finish (Table A-18). As shown in Figure 16, small ECEA angles improved the surface finish, with only one exception. For a case in which the nose radius of the tool is much less than the feedrate, the surface that is produced will appear similar to that shown in the top portion of Figure 17.[8] As indicated, the surface finish is primarily the result of the ECEA; the smaller the angle, the better will be the finish. Tools having an ECEA of zero have been used by some individuals to obtain good finishes in brass.[9]

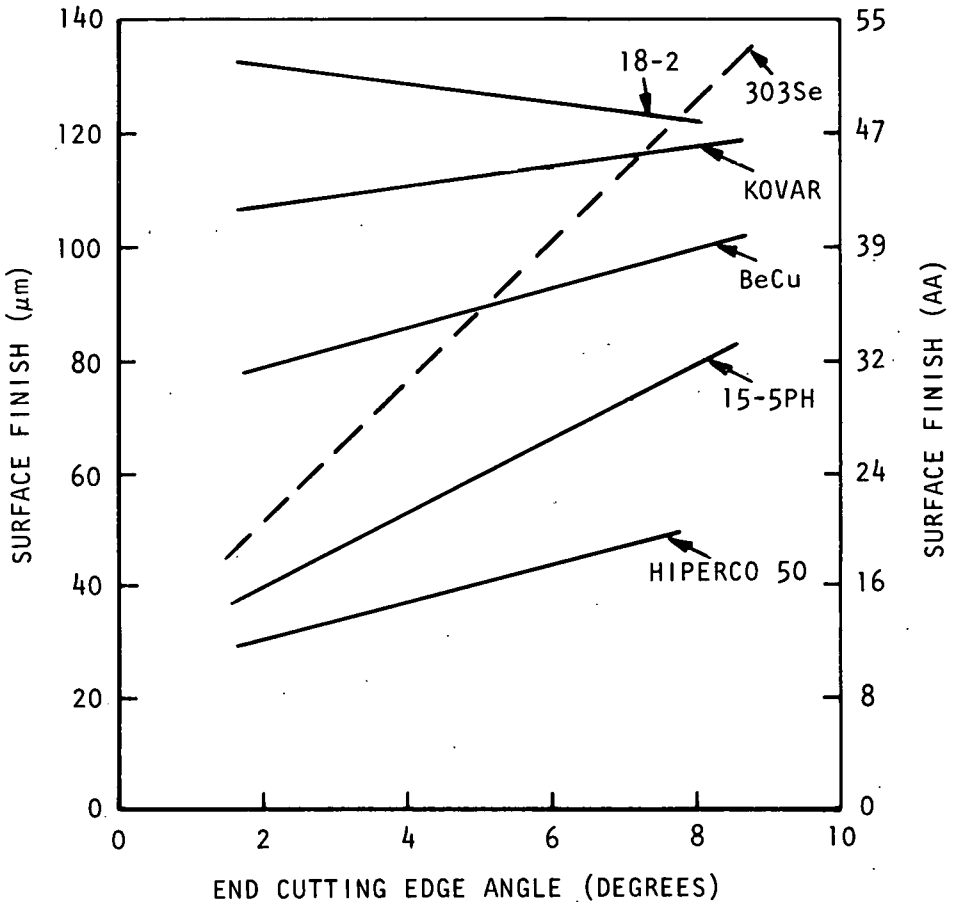

Figure 16. Surface Finish as a Function of ECEA

When the nose radius is equal to or larger than the feedrate, the surface that is produced will appear similar to that shown in the bottom portion of Figure 17.[8] As indicated, the ECEA has a negligible effect. In the tests that were made, both of the conditions shown in Figure 17 existed.

For a tool having an SCEA of nearly zero and an infinitely small nose radius, the *maximum* amplitude of the surface roughness (h) can be expressed by the following equation.

$$h = \frac{f}{\text{cotan (ECEA)}}, \qquad (8)$$

where

f = feedrate per revolution.

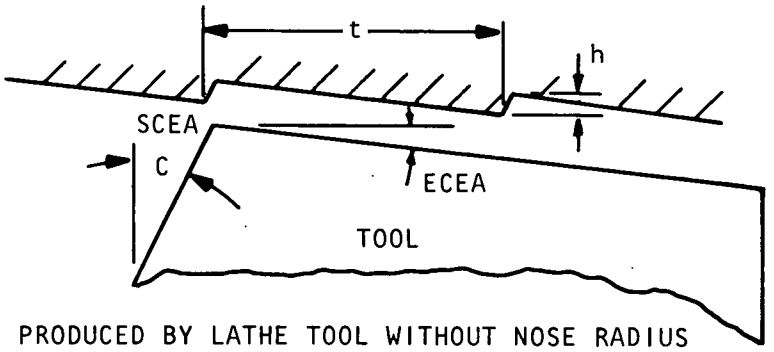

SURFACE PRODUCED BY LATHE TOOL WITHOUT NOSE RADIUS

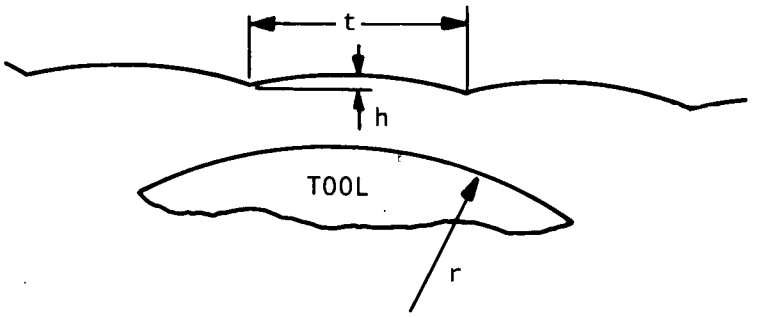

SURFACE PRODUCED BY LATHE TOOL HAVING CIRCULAR PLAN

Figure 17. Effect of Shape of Tool Nose on Surface Finish[9]

For a nose radius $R_N < f$,

$$h \simeq \frac{f^2}{8R_N}. \tag{9}$$

For $R_N > f$,

$$h_{rms} \simeq \frac{0.7f^2}{8R_N}. \tag{10}$$

More general equations have been developed by Shaw and Crowell[10] for theoretical surface finish as a function of nose radius, feedrate, SCEA, and ECEA.

For a 76.2-μm (0.003 inch) nose radius and a feedrate of 36.6 μm/revolution (0.00144 in./rev), Equation 10 predicts a surface finish of 1.524 μm (60 microinches). As shown in

Table 5, this is 50 to 100 percent higher than those that were actually measured.

Although Enache's work[11] indicates that back rake and end relief affect the surface finish of steel and cast iron, the results of this study do not show this to be valid for all metals. This apparent discrepancy probably is due to the relatively narrow range of angles that were used in this study; however, the choice of angles here used is consistent with production usage.

Burr Height

During machining operations, a burr is formed on the shoulder of any part that is faced or turned (Figure 18). A Poisson burr occurs when tools having positive SCEAs are used.[12] For a negative SCEA, the burr that is formed during the facing operation is actually a rolled-over chip. When the depth-of-cut is the same order of magnitude as the nose radius, the burr is formed by the combined action of lateral extrusion and chip roll-over.

In a previous study,[12] the SCEA, depth-of-cut, and feedrate were shown to be highly significant in determining the burr height in 303Se stainless steel. Again, the fact that that finding was not reaffirmed in this study (Table A-19) apparently is because of the narrow range of cutting conditions used in these tests. As shown in Table A-19, every factor and interaction affected the height of the burrs produced from Kovar.

Table 5 indicates that the burr height varied from 35.56 to 462.28 μm (0.0014 to 0.0182 inch) when the average of all cuts was taken. While the elongation of a workpiece is one key to the burr size, the strain-hardening exponent proved to be the best key in this study (Figures 19 and 20). While this result should be useful for turning and facing operations involving small depths-of-cut, it is not valid for facing long shoulders. In this case, "long" can be considered anything greater than 10 times the nose radius.

Burr Thickness

Previous tests in 303Se stainless steel[12] indicate that burr thickness, where the burr joins the parent workpiece, is a function of the SCEA, depth-of-cut, and feedrate. For depths-of-cut having the same magnitude as the nose radius, the SCEA should not have any noticeable influence. For the conditions used in this test, no factor influenced the burr thickness in all of the materials, and half of the materials were not affected by any factor (Table A-20).

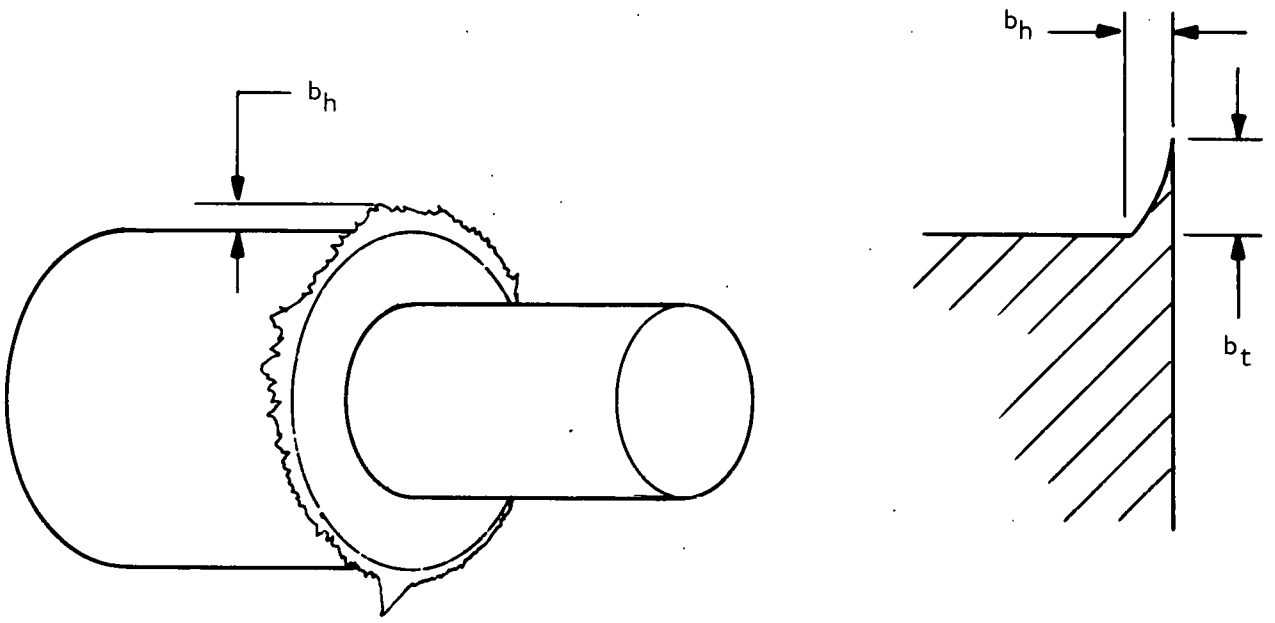

Figure 18. Location (Left) and Cross Section (Right) of a Burr Produced by Turning and Facing Operations

As shown in Table 5, burr thicknesses varied from 40.6 to 241.3 μm (0.0017 to 0.0095 inch) when average properties were calculated. As predicted by theory, burr thickness is a linear function of the strain-hardening exponent (Figure 20); it also appears to be related to workpiece elongation (Figure 19).

For miniature precision components, burr thickness must be kept to less than 76.2 μm (0.003 inch) in order to maintain part dimensions during the deburring operation. For very small parts having tolerances of ±5.1 μm (±0.0002 inch), burr thickness must be kept to less than 25.4 μm (0.001 inch). The thinner a burr, the easier it is to remove.

One reason that the ANOVA summaries for burr height and thickness (Tables A-19 and A-20) are relatively barren is that the variability of the burr size masked many of the trends which existed.

Unit Power

Although the cutting forces provide a good indication of metal-cutting efficiency, they generally are given for a specific feedrate and speed, and they do not provide a measure of the power required to produce a given cut. A knowledge of the required power is essential to the prevention of machine overloading during heavy cuts. While this knowledge is not critical

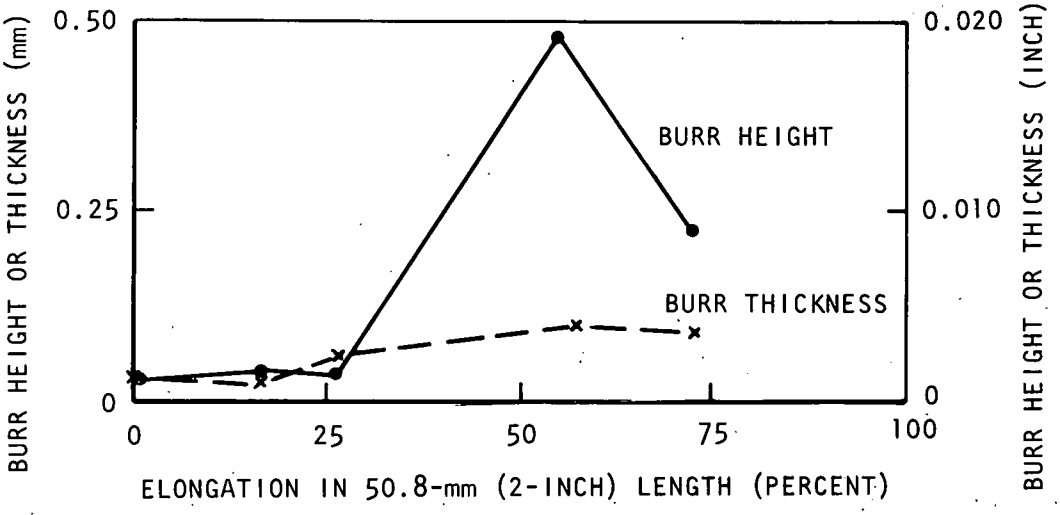

Figure 19. Effect of Elongation on Burr Height and Thickness

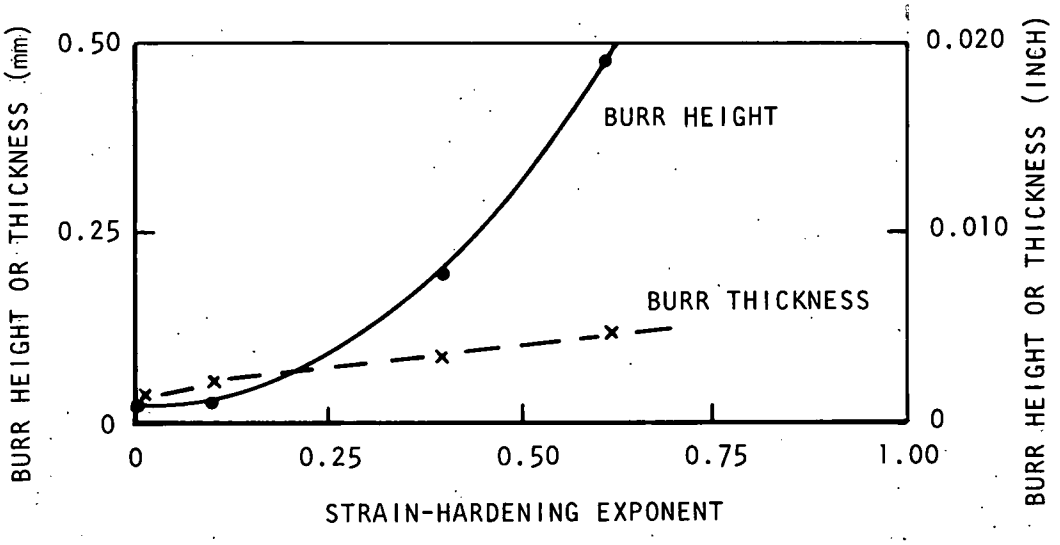

Figure 20. Effect of Strain-Hardening Exponent on Burr Height and Thickness

for finishing cuts, it provides a universally appreciated measure of the cutting difficulty.

For comparison purposes, the unit power (W_N), rather than the actual power, generally is given. Unit power is the horsepower per cubic inch of metal removed per minute. For a turning operation, it can be calculated from the following equation.

$$W_N = \frac{hp}{12dfV} = \frac{F_T}{396{,}000\ df}, \qquad (11)$$

where

F_T = the principal cutting force (Figure 6) in pounds,

d = the radial depth-of-cut in inches,

f = the feedrate (IPR), and

V = the surface velocity (SFPM).

The values of W_N that were calculated for this study are considerably larger than the typical values that are given in handbooks (Table 6). This is the direct result of using low feedrates. While W_N is relatively independent of feedrate at rates exceeding 101.6 μm/revolution (0.004 ipr), it is notably affected at rates below this value. Figure 21 illustrates the trend in 303Se stainless steel; this graph is based on the data shown in Figure 12.

When handbook values are used to calculate the cutting force, the results will be considerably less than the measured forces if low feedrates are involved. Because of the wide range of hardness values that are available for some metals, the values will differ notably from handbook values; handbook values are based on a single hardness value for a given metal.

Tool Wear and Its Effects

Tool wear was monitored to determine whether conventional definitions of tool life have any correlation with the parameters that were of interest in this study. In addition, a knowledge of the influence of tool wear upon the observed results was desired.

Because tool wear was expected to be less than that which normally is encountered in conventional machinability tests, it was only checked after all of the specimens had been produced. Since each tool produced only 2 or 10 specimens, only one group of readings was obtained for each set of machining conditions. The obtained values that were based on the machining of 10 specimens have been previously reported.[1]

The tool properties that were measured included the nose-radius change, the radial wear, and three values of the flank-wearland width. The wearland at the nose, the uniform wearland, and the localized wear at the point where the maximum diameter of the stock touched the tool were recorded (Figure 22). Wearland measurements which indicate the end of tool life in conventional tests are shown in Table 7.

Table 6. Unit Power (W_N) Values

Material	Unit Power: Experimental Values: Average* ($W/cm^3/s$; $HP/in.^3/min$)	Unit Power: Experimental Values: Tool 1** ($W/cm^3/s$; $HP/in.^3/min$)	Unit Power: Handbook Value*** ($W/cm^3/s$; $HP/in.^3/min$)
303Se	4.0 (5.3)	2.7 (3.5)	1.0 (1.3)
15-5PH	2.4 (3.1)	1.8 (2.3)	1.1 (1.4)
BeCu	1.2 (1.6)	0.8 (1.1)	0.8 (1.0)
Kovar	1.9 (2.6)	1.4 (1.9)	1.5 (2.0)
Hiperco	3.6 (4.7)	2.5 (3.3)	1.9 (2.5)
18-2	1.6 (2.1)	2.3 (3.0)	1.0 (1.3)

*Average values based on 16 tools.
**Values obtained from Tool 1 which typically produced the lowest W_N values.
***Traditional-unit values from *Machining Data Handbook.*[13]

The average wearland heights that were observed in this test are considerably less than those normally used to define the end of tool life (Table A-22 and Figures 23 and 24). Since the objective of this study was to describe conditions for which radii in the order of 50.8 to 76.2 μm (0.002 to 0.003 inch) can be maintained, and since the average radius produced was 71.1 μm (0.0028 inch, Table 5), the values shown in Figures 23 and 24 represent the maximum that can be used to define tool life. No obvious correlation was observed between the wearland height and the other variables.

As a general rule, the cutting tools had a nose radius from 25.4 to 76.2 μm (0.001 to 0.003 inch) after 0.29 m (11.25 inches) of cut. Little additional wear occurred after 1.428 m (56.25 inches) of cut. As shown in Figure 25, the wearing of the tool from a sharp point to a radius causes a shortening (δ) of the tool where

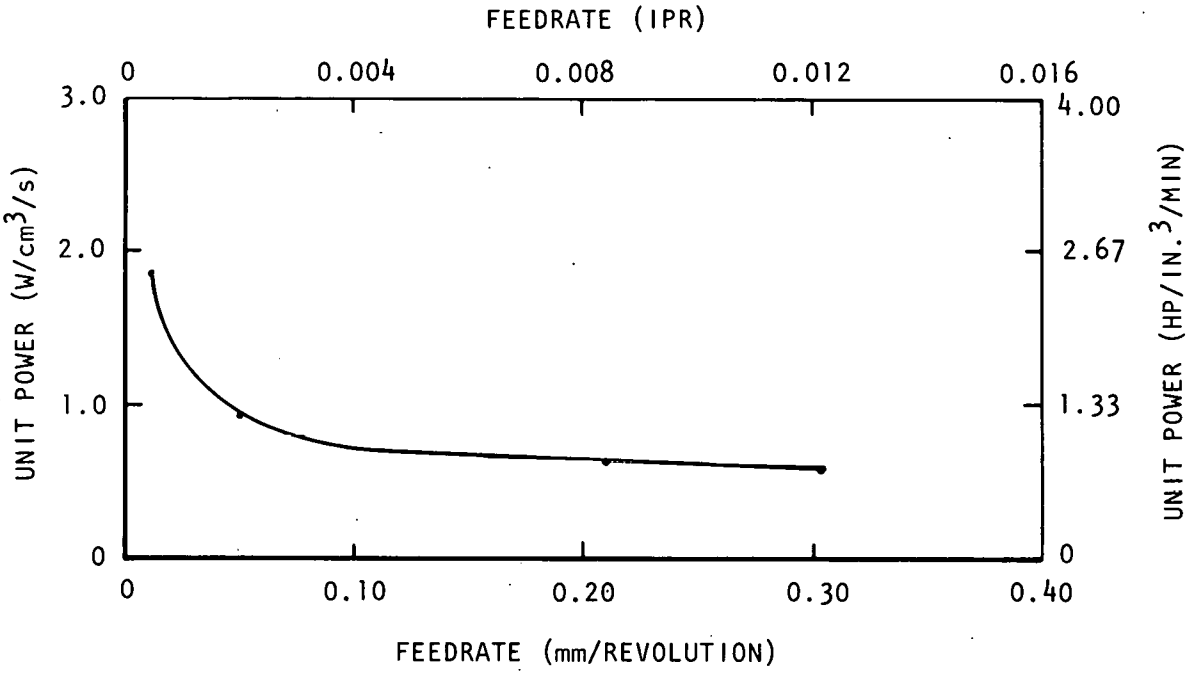

Figure 21. Effect of Feedrate on Unit Power for HSS Tool in Cold-Rolled 303Se Stainless Steel

$$\delta = r\left(\frac{\cos \theta}{\sin \phi - 1}\right), \tag{12}$$

$$\theta = \frac{90 - SCEA - ECEA}{2}, \tag{13}$$

and

$$\phi = \frac{90 + SCEA - ECEA}{2}. \tag{14}$$

Note that the negative sign for a negative SCEA must be inserted in these equations to obtain proper results. For an SCEA of -8 degrees, an ECEA of 7 degrees, and a radius of 76.2 μm (0.003 inch), the wear (δ) predicted by Equation 12 is 86.4 μm (0.00034 inch).

As a general rule, the measured nose radius of the tool at the end of the test was nearly the same as the fillet radius that had been produced on the part. Some differences occurred, however, because of a buildup of material on the cutting edge and nonuniform point fractures and wear.

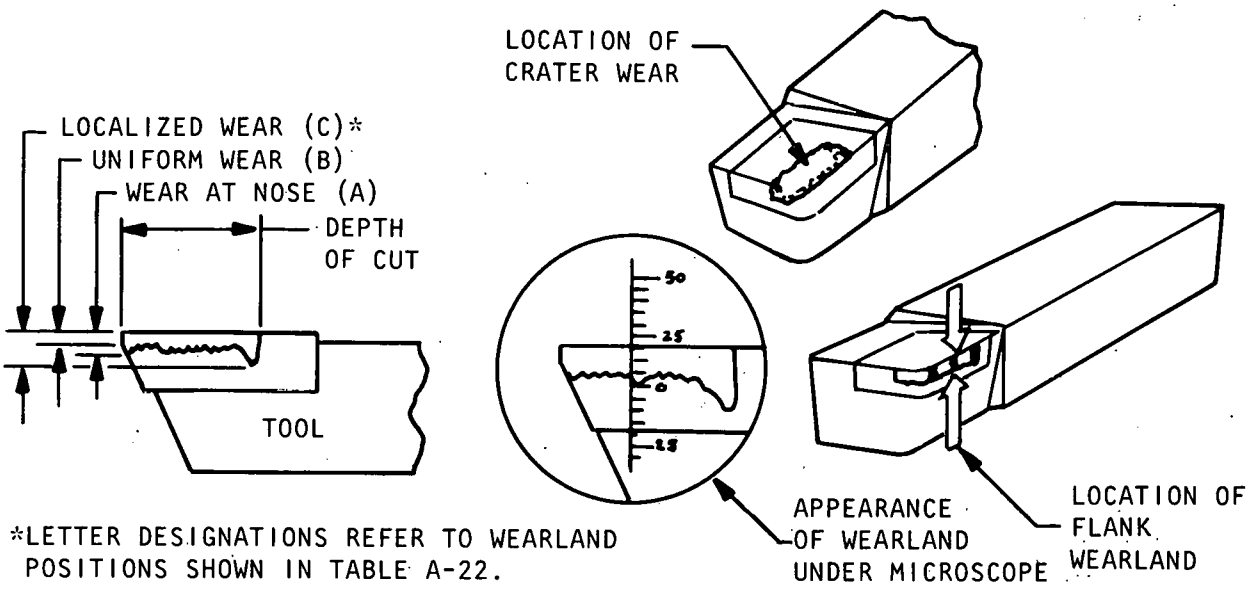

Figure 22. Wearland Measurements Made for Tool-Life Testing

Table 7. Tool-Life End Points Commonly Used in Machinability Testing

Operation	Tool Material	Flank Wear			
		Average		Maximum Local	
		(mm)	(Inch)	(mm)	(Inch)
Turning	HSS	1.52 A*	0.060	1.52 A	0.060**
	Carbide	0.38	0.015	0.76	0.030
Face Milling	HSS	0.76†B	0.030	0.76 B	0.030
	Carbide††	0.38	0.015	0.76	0.030
End Milling: Slotting	HSS	0.30 B	0.012	0.51 B	0.020
	Carbide	0.30	0.012	0.51	0.020
End Milling: Peripheral	HSS	0.30 B	0.012	0.51 B	0.020
	Carbide	0.30	0.012	0.51	0.020
Drilling	HSS	0.38 C	0.015	0.38 C	0.015
	Carbide	0.38	0.015	0.38	0.015
Reaming	HSS	0.15 D	0.006	0.15 D	0.006
	Carbide	0.15	0.006	0.15	0.006
Tapping	HSS	Go No-Go Gage		Tap Fracture	

*A = measured on flank; B = measured on primary clearance; C = measured on lips of drill point; and D = measured on lead chamfer.
**Nose breakdown or 1.52 mm (0.060 inch), whichever occurs first.
†Multiple-tooth.
††Indexable.

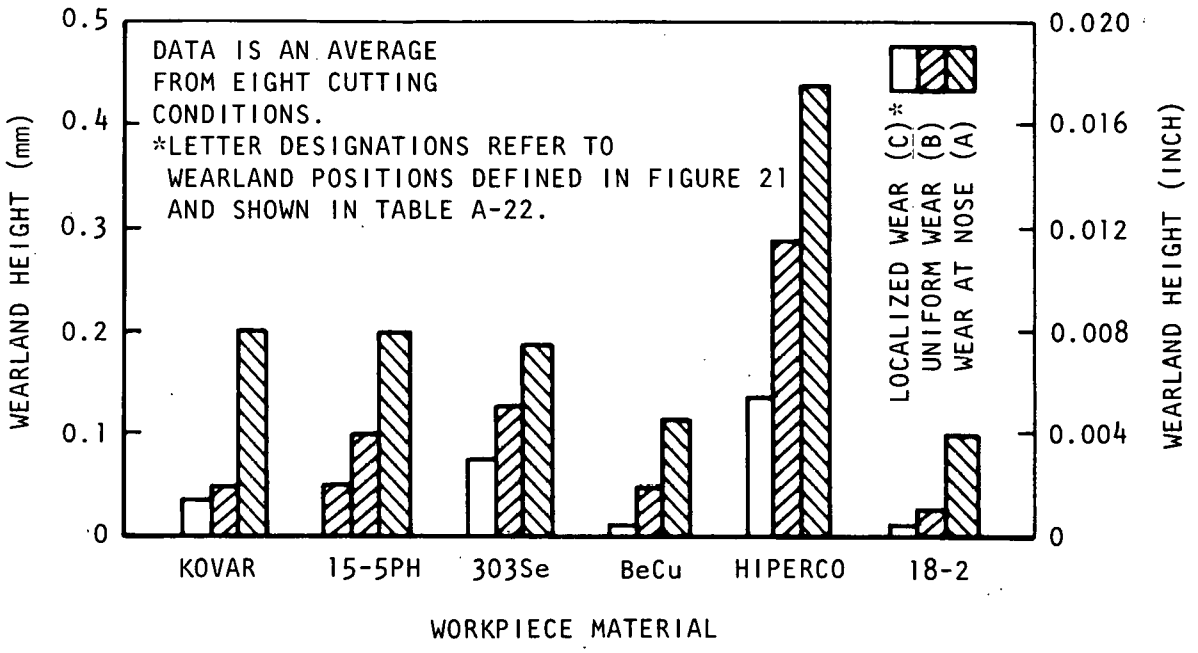

Figure 23. Wearland Heights After 0.29 m (11.25 Inches) of Axial Cut

Actual measurements of the radial tool wear (δ, or the physical length of the tool which was worn away) were in the order of 25.4 μm (0.001 inch). As a general rule, the radial tool wear was less than 25.4 μm (0.001 inch) after 0.29 m (11.25 inches) of cut, and 55.9 μm (0.0022 inch) after 1.428 m (56.25 inches) of cut. Figure 26 shows the tool wear that occurred in two materials that are common to the manufacture of miniature precision parts.

Effect of Length-Of-Cut on Variables

Of the 280 combinations of variables that were investigated in which 10 specimens were produced by each tool, 59 changed as additional samples were machined. The change was of the form shown by the following equation.

$$Y = a_1 + a_2X, \qquad (15)$$

where

Y = surface finish, burr size, cutting forces, or other variable,

a_1 = a constant,

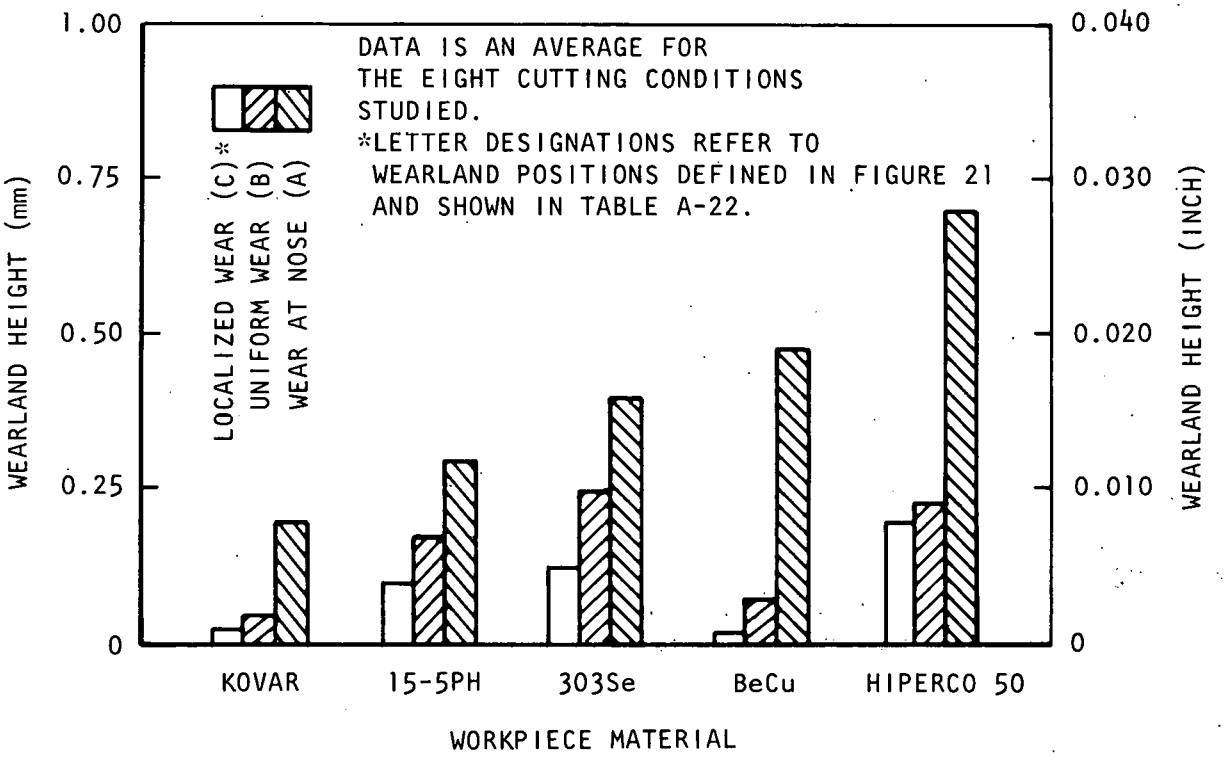

Figure 24. Wearland Heights After 1.428 m (56.25 Inches) of Cut

a_2 = a constant, and

X = number of specimens machined.

This equation can be made more explicit, as illustrated by Equations 16 and 17, by substituting the inches-of-cut or the time-in-cut for each specimen.

$$Y = a_1 + a_2\left(\frac{T}{0.432}\right), \tag{16}$$

and

$$Y = a_1 + a_2\left(\frac{L}{5.625}\right), \tag{17}$$

where

T = the time-in-cut, in minutes, and

L = the length-of-cut, in inches.

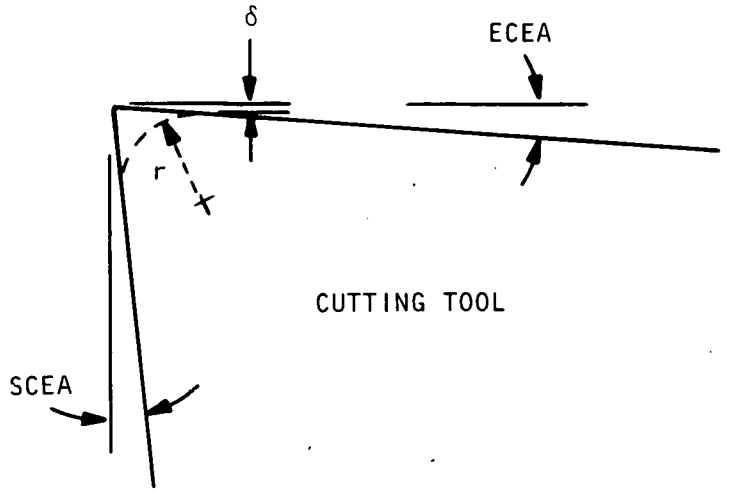

Figure 25. Shortening of Tool Produced by Radius-Generating Wear

The constants a_1 and a_2 for the combinations in which linear trends were found to exist are presented in Table A-23. The only obvious trend was that the fillet radius did not vary as a function of the cutting time. In general, the conclusion must be reached that tool wear only slightly affected the measured properties. As shown in Table A-23, certain tools did exhibit wear in some specific materials.

Results Ranked As a Function of Tool Geometry

As previously indicated, the results obtained from one material were often notably different from those obtained from another material. Although this information is significant, defining tools which were optimum in all (or most) materials is more meaningful.

The best tool geometry and cutting conditions that were used in the tests can be defined by ranking the best and worst conditions. "Best," as here defined, indicates the smallest radius, burr thickness, or length, and the lowest numerical value of surface roughness. Cutting forces are not included in this ranking since they are a function of the depth-of-cut. By assigning a "+1" to the two tools producing the best results and a "-1" to the two tools producing the worst results, a numerical value of the tool performance can be obtained.

Using the described approach, Tools 3 and 10 were found to be generally more desirable than the others; Tools 4 and 5 were

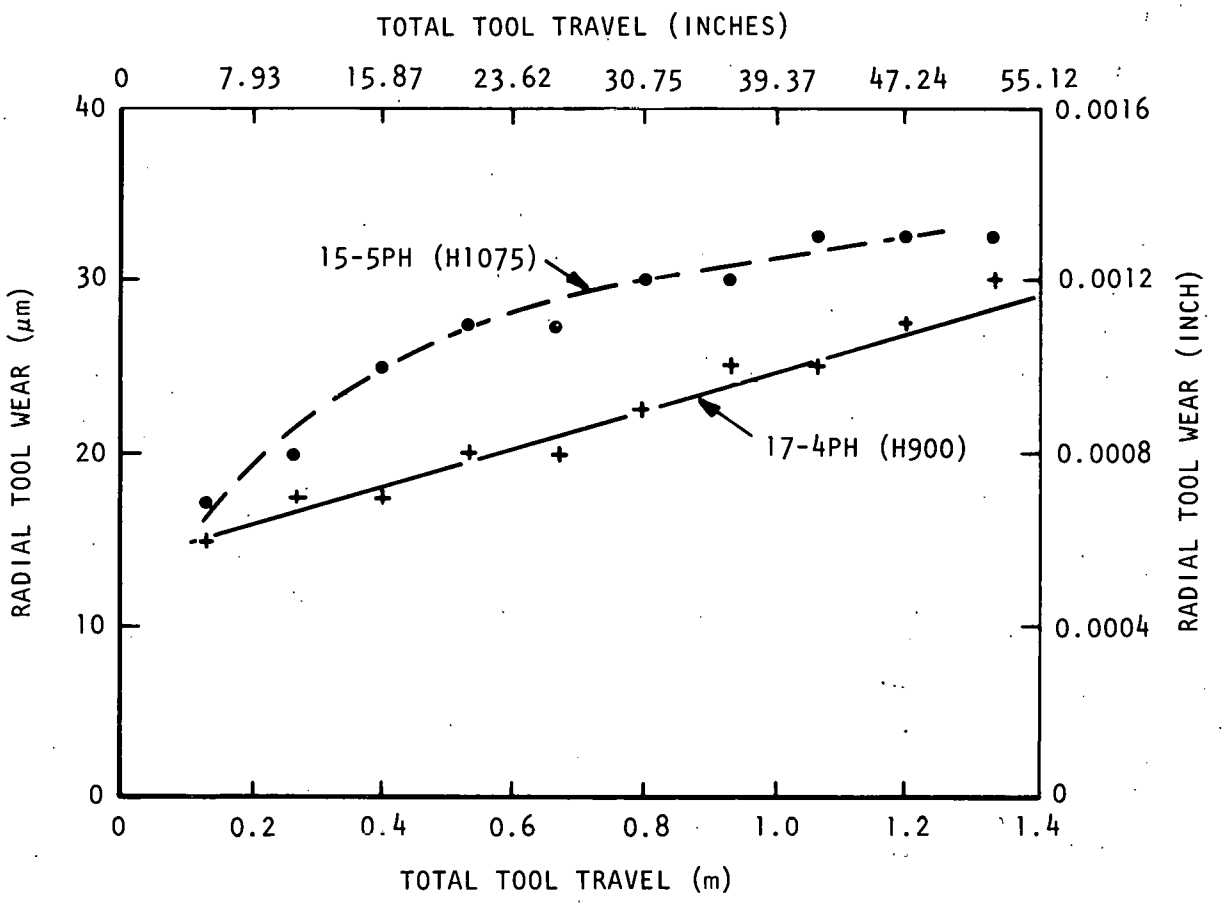

Figure 26. Radial Tool Wear as a Function of Length-Of-Cut

found to be less desirable. Tool 3 was characterized by a high ECEA and side rake angle; Tool 10 had a low ECEA. Tools 3 and 10 both had low end relief angles, high side rake angles, and high back rake angles. Tools 4 and 5 had low side rake angles, and the values of the SCEAs were more negative than those on Tools 3 and 10.

Results Compared to Published Recommendations

In general, the tool angles that are recommended in published sources closely approximate those that were found to be optimum in these tests (Table 8). This implies that finish-cut tools need be no different than the tools that are normally used. The only exception to this statement is the back rake angle; a 5-degree back rake angle performed better than a 0-degree angle.

Table 8. Comparison of Commercially Recommended and Empirically Determined Optimum Tool Angles*

Material	Tool Angle					
	BR (Degrees)	SR (Degrees)	ERf (Degrees)	SRf (Degrees)	SCEA (Degrees)	ECEA (Degrees)
303Se and 18-2						
Handbook**	0	10	5	5	15	15
Experiment	5	10	5		-2	7
15-5						
Handbook**	0	10	5	5	15	15
Experiment	5	10	5		-2	7
BeCu						
Handbook**	5	10	8	8	5	5
Experiment	5	10	5		-2	7
Handbook***	0 to 10	10	5	5	0 to 15	5
Kovar						
Handbook†	12 to 14	12 to 14	10 to 12	8		
Experiment	5	10	5		-2	7
Hiperco 50						
Handbook††						
Experiment	7	10	0		-2	7

*For HSS tools.
**_Machining Data Handbook._[13]
***Kawecki Berylco Industries, Inc.[14]
†_Machining Nickel Alloys._[15]
††Data not available.

Results Ranked by Material, Using Optimum Tool Geometry

When the workpiece materials are ranked by the results obtained, the materials having the lowest elongations obviously produced shorter and thinner burrs (Table 9). Although the data indicated that these same materials also tended to produce a better surface finish, that effect was partially the result of a larger tool radius being formed on the tools that were used in these materials. The data for fillet radius, for example, illustrate that Hiperco formed a large tool radius.

By rearranging Equation 9, the product of the surface finish and the tool-nose radius can be seen to be a constant for a given tool geometry, feedrate, and material. The larger the constant, the worse will be the finish for a given nose radius. The constant for each material is the last variable shown in Table 9. Estimates of the surface finish produced by a 50.8-μm (0.002 inch) nose radius are shown in Table 10.

Tool forces were roughly proportional to the workpiece hardness. This is in agreement with published information on cutting forces.

From a production standpoint, machinability is defined as the frequency of tool change. Since tools are changed for all of the first four reasons shown in Table 2, tool life would be defined as the point at which the tool was changed because it was exceeding any one of the stated limits. Table 11 shows the results, based on Tool 3 cutting 10 samples.

While this approach provides a realistic technique for evaluating machinability, it too is limited by the conditions that are chosen to indicate the end of tool life. Because wear patterns slow down after the initial wear, increasing the end-of-life conditions by 50 percent may substantially change the relative machinability relationships. For example, by increasing the allowable fillet radius or the burr size by 50 percent, most of the materials that were studied would have relatively equal machinability-index numbers. The 18-2 material is not shown in Table 11 since only 286 mm (11.25 inches) of cut were made. Based on its performance, with the exception of the surface finish produced, it would rank just below Hiperco 50.

The results shown in Table 11 are not as negative as they might at first appear. Slowing the feedrate by a factor of 4 would improve the surface finish produced on all materials by approximately the same ratio. This action of course would slow production by a similar amount. Allowing larger fillet radii also would improve the surface finish, as would the use of ECEAs of nearly zero.

Table 9. Results Ranked by Material, Using Optimum Tool Geometry

Measured Variable and Measuring Units	Material Ranking					
	Best	Better	Fair	Poor	Worse	Worst
Fillet Radius	18-2	303Se	BeCu	15-5PH	Hiperco	Kovar
μm	35.6	35.6	48.3	53.3	55.9	58.4
Inches x 10^{-4}	14	14	19	21	22	23
Surface Finish, AA	Hiperco	15-5PH	18-2	BeCu	Kovar	303Se
μm	0.30	0.58	1.22	1.22	1.40	1.47
Microinches	12	23	48	48	55	58
Recommended Cutting Speed	BeCu	18-2	Kovar	303Se	Hiperco	15-5PH
mm/s	1275	1122	729	510	306	245
SFPM	250	220	143	100	60	48
Cutting Force F_T	BeCu	18-2	Kovar	15-5PH	303Se	Hiperco
N	17.8	31.1	31.1	44.5	53.4	53.4
Pounds	4	7	7	10	12	12
Burr Length	15-5PH	BeCu	18-2	Hiperco	Kovar	303Se
μm	0	15.2	33.0	35.6	45.7	243.8
Inches x 10^{-4}	0	6	13	14	18	96
Burr Thickness	15-5PH	BeCu	18-2	Hiperco	Kovar	303Se
μm	0	30.5	33.0	33.0	66.0	96.5
Inches x 10^{-4}	0	12	13	13	26	38
Surface Finish x Fillet Radius	Hiperco	15-5PH	18-2	303Se	BeCu	Kovar
μm^2	16.8	30.9	43.4	52.3	58.9	81.8
Inches^2 x 10^{-10}	264	483	576	812	912	1265

Table 10. Surface-Finish Predictions for 50.8-μm (0.002 inch) Nose Radius on Tool 3

Material	Estimated Surface Finish	
	μm AA	Microinches AA
Hiperco	0.33	13
15-5PH	0.61	24
18-2	0.71	28
303Se	1.04	41
BeCu	1.17	46
Kovar	1.60	63

Because tolerances generally can be controlled by frequent tool adjustments, including radial tool wear in the machinability index is unrealistic. Table 12 shows the amounts of wear that were observed on Tool 3 after 1.429 m (56.25 inches) of cut.

When tolerances cannot be maintained because the small diameter of the workpiece permits it to be bent by the cutting forces, the ratio F_T/E, where E is the modulus of elasticity, becomes significant since it is proportional to the deflection of the part. Table 13 illustrates the average values that were found for Tool 3, based on average forces from the two samples studied. As shown, when machining was performed under the conditions used in this study, Hiperco 50 parts deflected almost twice the distance that beryllium-copper parts did; this resulted in twice the taper on the Hiperco 50 parts.

Predicting Optimum Tool Geometry and Performance

One of the principal objectives of this study was to develop equations for optimizing tool geometry and predicting tool performance. Two approaches have been used to obtain these equations: (1) when equations that had been developed from theoretical considerations were known, they were used with any modifications of the constants that might be required; (2) when such relationships were not known, linear-regression techniques were employed to establish the desired predicting equations. Equation 11 is an example of the first approach, and Equations 2 through 7 are examples of the second.

Table 11. Machinability Index Using the First Constraint Exceeded by Tool 3 as the End-Of-Life Point

Material	Machinability Index: Time in Cut (Minutes)	Machinability Index: Length of Cut, m	Machinability Index: Length of Cut, Inches	Constraint Exceeded
15-5PH	130	1.429	56.25	None
Hiperco	39	0.429	16.88	Nose Radius
Kovar	0	0	0	Surface Finish
BeCu	0	0	0	Surface Finish
303Se	0	0	0	Finish/Burr

In determining the optimum tool geometry, both of the described approaches must be used. As noted by Shaw,[8] while the side rake, the back rake, and the other tool angles describe the tool geometry, four other related angles better describe the cutting effects. These angles, discussed in detail by McGee and others,[16] include the inclination angle (AI), the velocity rake angle (AV), the normal rake angle (AN), and the effective rake angle (AE). They are calculated from the following formulas.

$$AV = \tan^{-1}[\tan(SR)\cos(SCEA) + \tan(BR)\sin(SCEA)] \quad (18)$$

$$AI = \tan^{-1}[\tan(BR)\cos(SCEA) - \tan(SR)\sin(SCEA)] \quad (19)$$

$$AN = \tan^{-1}[\tan(AV)\cos(AI)] \quad (20)$$

$$AE = \tan^{-1}[\tan(SR)\cos(SCEA+AI) + \tan(BR)\sin(SCEA+AI)] \quad (21)$$

From geometry considerations, as indicated by McGee and others:[16]

$$\sin(AE) = \sin^2(AI) + \cos^2(AI)\sin(AN). \quad (22)$$

Thus if any two of the three angles AI, AN, or AE are known, the third can be calculated. Furthermore, if two of these angles can be defined as functions of workpiece-material properties, then all basic tool angles (SCEA, BR, SR) can be determined as functions of material properties through the use of Equations 18 through 22.

McGee[17] has developed regression equations from which AN and AI can be calculated from a knowledge of only workpiece properties.

Table 12. Radial Wear of Tool 3 After 1.429 m (56.25 Inches) of Cut

Material	Radial Tool Wear, μm	Radial Tool Wear, Inch	Ranking by Tool Wear
15-5PH	50.8	0.0020	3
Hiperco	78.7	0.0031	5
Kovar	25.4	0.0010	1
BeCu	61.0	0.0024	4
303Se	35.6	0.0014	2

In his study, conditions were selected which provided the highest metal-removal rate for a 60-minute tool life using carbide tools. AN and AI were calculated for the tools, and regression equations then were developed which related AN and AI to the workpiece properties.

A similar approach was used in this study: optimum values of AI and AN first were selected from the experimental results obtained from the 10 samples studied. (Optimum was defined as the geometry which provided the smallest fillet radius, burr thickness, burr length, etc.) These values then were fitted to the following equation to provide values for the "A" constants.

$$AI = A_1 + A_2\text{yield} + A_3\text{tensile} + A_4\text{elongation} + A_5 n, \qquad (23)$$

where

yield = yield strength of the workpiece material,

tensile = tensile strength of the workpiece material,

elongation = elongation occurring in a 50.8-mm (2-inch) gage-length tensile specimen,

n = strain-hardening exponent, and

AI = the inclination angle, expressed in degrees.

Table 14 presents the constants that were determined from these data. Note that since the optimum was defined by 11 different

Table 13. F_T/E Ratios for Average Results From Tool 3

Material	F_T/E mm^2	F_T/E $Inches^2 \times 10^{-7}$	Ranking by F_T/E
15-5PH	0.022	3.4	3
Hiperco	0.026	4.0	5
Kovar	0.023	3.5	4
BeCu	0.014	2.2	1
303Se	0.026	4.1	6
18-2	0.016	2.5	2

criteria, 11 different sets of constants are required. Theoretically, the angle AI which helps maintain the smallest fillet radius, burr thickness, etc, can be calculated from a knowledge of only these constants and the workpiece properties. Because only five materials were studied and five constants had to be calculated (18-2 was not studied), the accuracy of the equation could not be determined.

McGee has established relationships between the machining shear strength, the yield strength, the strain-hardening exponent, and the optimum effective rake angle.[17] However, using the procedures that he has described, the reproduction of his results from the material properties used in this test proved impossible. The major discrepancy occurred for Hiperco 50, which is the only brittle material of those studied. The fact is apparent, however, that some relationship exists in ductile materials between the strain-hardening exponent, the minimum machining shear stress, and the tool geometry.

An observation of the conditions that produced the minimum measured value of each variable demonstrates two trends (Table 15). First, from production experience, the fillet radius and the surface finish generally are improved by keeping the nose area of the tool strong. This is accomplished by minimizing the rake angles. Some of this trend is illustrated in Table 15.

Second, the cutting force, unit power, and burr size are minimized by using large rake angles in order to minimize the cutting-stress field. This, too, is demonstrated by a large AE angle. Hiperco 50, however, does not follow the pattern of the ductile materials.

Table 14. Constants for Dependent Variables

Dependent Variable	Constants*				
	A_1	A_2	A_3	A_4	A_5
Fillet Radius	-5.07670	2.49945	-2.35040	-2.52382	731.64138
Surface Finish	3.49018	-2.19141	2.11381	2.05471	-623.61309
Burr Length	11.43069	-2.12451	1.98890	2.05779	-606.25984
Burr Thickness	-25.11961	10.63878	-9.95910	-10.34660	3035.92569
F_R	-52.62857	19.21014	-18.01917	-18.20758	5453.61553
F_T	-28.72118	9.37876	-8.74708	-8.87247	2659.71250
F_A	-55.87274	19.90027	-18.65057	-18.98760	5667.29570
Wearland A	-53.98522	22.47578	-21.11286	-21.72897	6425.97376
Wearland B	-20.97910	10.16035	-9.56164	-9.77064	2904.16330
Wearland C	9.00749	-0.94622	0.88650	0.92638	-272.81618
Radial Wear	14.77606	-4.83612	4.52406	4.63526	-1366.17816

*Substitute horizontal row of constants shown into Equation 23 to determine angle AI which will minimize indicated variable.

Table 15. Values of Angle AE for Optimum Levels of Several Variables

Variable	Test Level	Angle AE (Degrees)	Material				
			303Se	15-5PH	BeCu	Kovar	Hiperco
Fillet Radius	121122	10.27	X*				
	112222	5.00		X	X	X	
	222112	9.93					X
Surface Finish	211212	4.79	X	X			
	222112	9.93			X		
	212121	10.00				X	X
Force F_T	121122	10.27	X	X	X	X	
	112222	5.00					X
Unit Power	111111	9.86	X	X		X	
	212121	10.00			X		
	122211	4.96					X
Burr Length	121122	10.27	X	X	X		X
	111111	9.86				X	
Burr Thickness	121122	10.27	X	X	X		X
	212121	10.00				X	

*X indicates the optimum tool geometry for the indicated material.

Although a regression equation of the following form can be established, there is little need to do so since the results are grouped in essentially only two groups of angle AE.

$$AE_{Opt} = A_1 + A_2\left(\frac{n}{yield}\right). \qquad (24)$$

For optimum fillet radius, angle AE should be 5 degrees; for force, power, and burr size, it should be 10 degrees. Thus by using one of these values of AE, evaluating AI from material properties (using Equation 23 and Table 14), substituting these values into Equation 22, arbitrarily selecting a value of SCEA, and substituting all of these values into Equations 19 and 21, the optimum back rake and side rake angles can be obtained. As previously mentioned, the tool angles that were optimum for most cases were close to the angles that are recommended in most handbooks; thus little purpose will be served by making all of the substitutions described.

An attempt also was made to fit each of the measured variables to the following equation.

$$Y = AI\left(A_1 + A_2 yield + A_3 tensile + A_4 elongation + A_5 n\right). \qquad (25)$$

Statistically, there was no fit to any of the seven principal measured variables.

A similar fit was tried with the depth-of-cut and angles AV, AN, AE, and AI as multipliers of constants A_1, A_2, and A_3. In this case, the following equation was tried.

$$Y = d\left[A_1 + A_2(AV) + A_3(AV)^2\right]. \qquad (26)$$

Again, none of the principal variables, the three wearland variables, or the radial wear fitted this equation.

Miscellaneous Tests

Three additional brief tests were performed on the materials listed in Table 3 to study the effects of feedrates, speeds, and of grooving and cutoff operations. In the first of these tests, ten specimens (as shown in Figure 7) were produced at different speeds and feedrates using both sharp and dull tools. The two dull tools were dulled by vibratory deburring them from 1/2 to 2 hours in 6.35-mm (0.25 inch) plastic pyramids.

As shown in Figure 27, low spindle speeds reduced the cutting forces noticeably at low feedrates, but they produced little

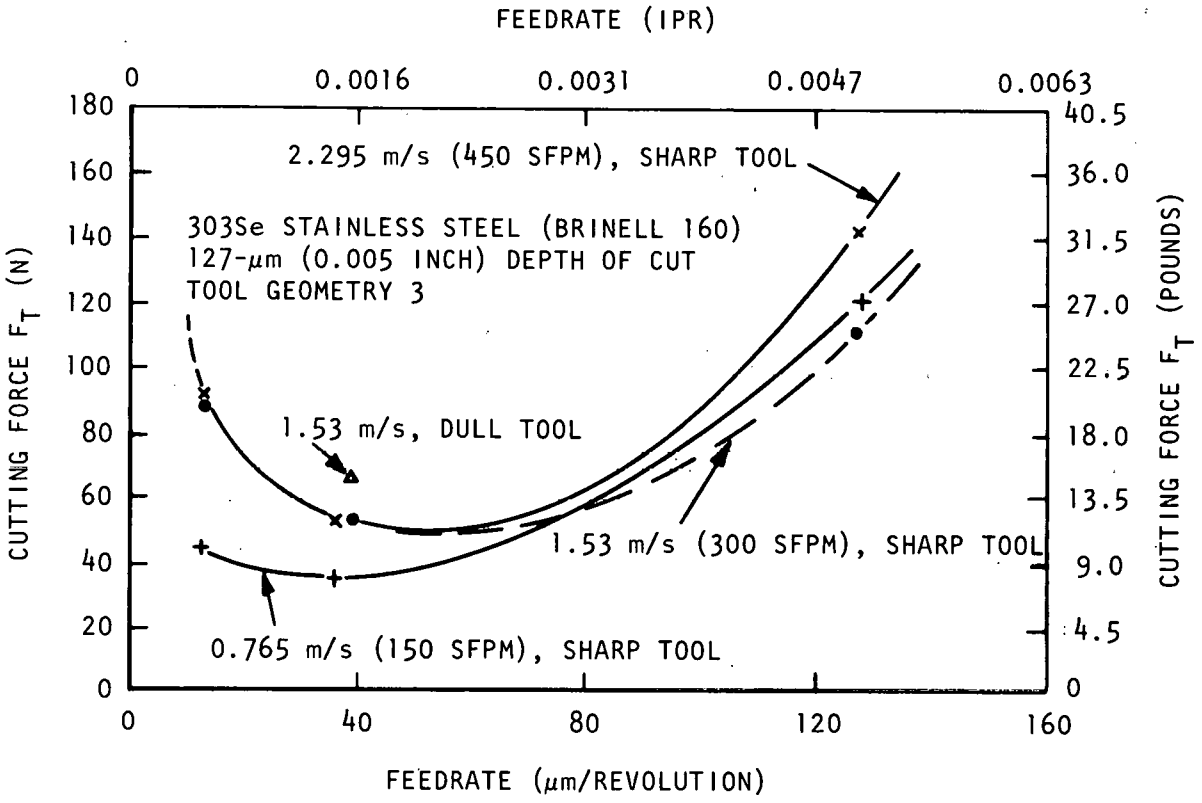

Figure 27. Effect of Feedrate and Spindle Speed on Cutting Force F_T

change at high feedrates in the annealed 303Se stainless steel. Figure 12 indicates that the effect of feedrate should be linear in the cold-rolled condition. The two dull tools increased F_T by only 13.3 N (3 pounds). The test data for other forces and parameters are shown in Table A-24.

As indicated in Figure 28, slowing the feedrate increases the burr thickness at spindle speeds exceeding 1.53 m/s (300 sfpm). This is a significant observation, since the burr size can be decreased 50 percent by slowing the feedrate. Dull tools increased the burr thickness by a factor as great as 5.0.

Burr heights increased slightly as the feedrates were reduced until a feedrate of 35.6 μm/revolution (0.0014 ipr) was reached; further reductions in the feedrate decreased the burr height.

The surface finish (and the product of the surface finish and the tool-nose radius) became worse as the feedrate increased above 35.6 μm/revolution; they also became worse as the feedrate was reduced below this value (Figure 29).

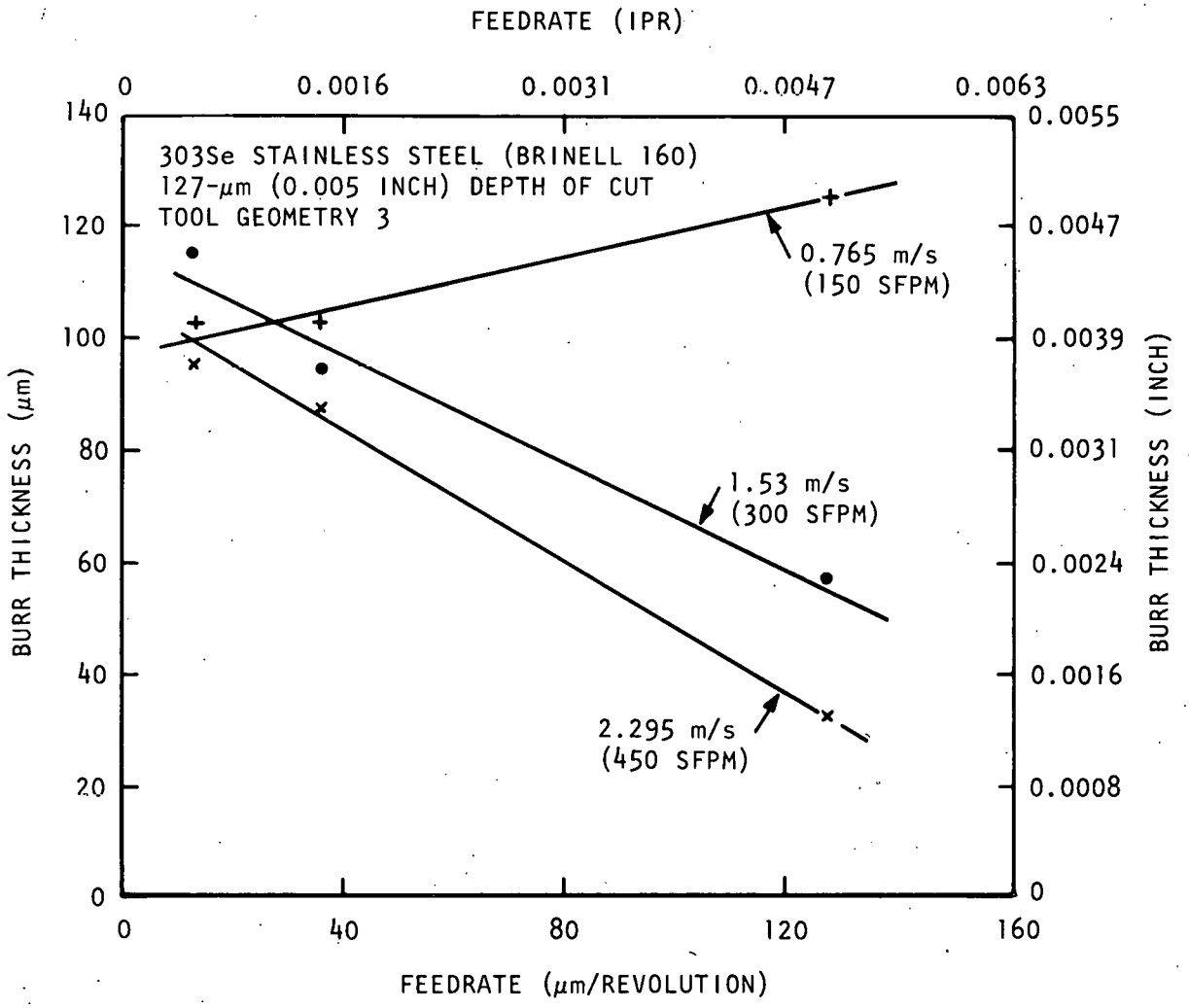

Figure 28. Effect of Feedrate and Spindle Speed on Burr Thickness

One-hundred grooves were cut in the diameter of the 18-2 and the 17-4PH stainless steels, and the fillet radius and burr size were monitored on each. No tool-wear trends were observed on a 0.75-mm-wide (0.030 inch) tool made from Carmet CA-310 carbide. A feedrate of 37.6 μm/revolution (0.0015 ipr) was used with a spindle speed of 300 rpm. Each tool produced a 0.635-mm-deep (0.025 inch) groove having a typical fillet radius of 50.8 μm (0.002 inch). Typical burrs were 38.1 μm high by 76.2 μm thick (0.0015 by 0.0030 inch). The burrs from 17-4PH stainless steel were slightly shorter, and they were only 59.7 μm (0.0023 inch) thick.

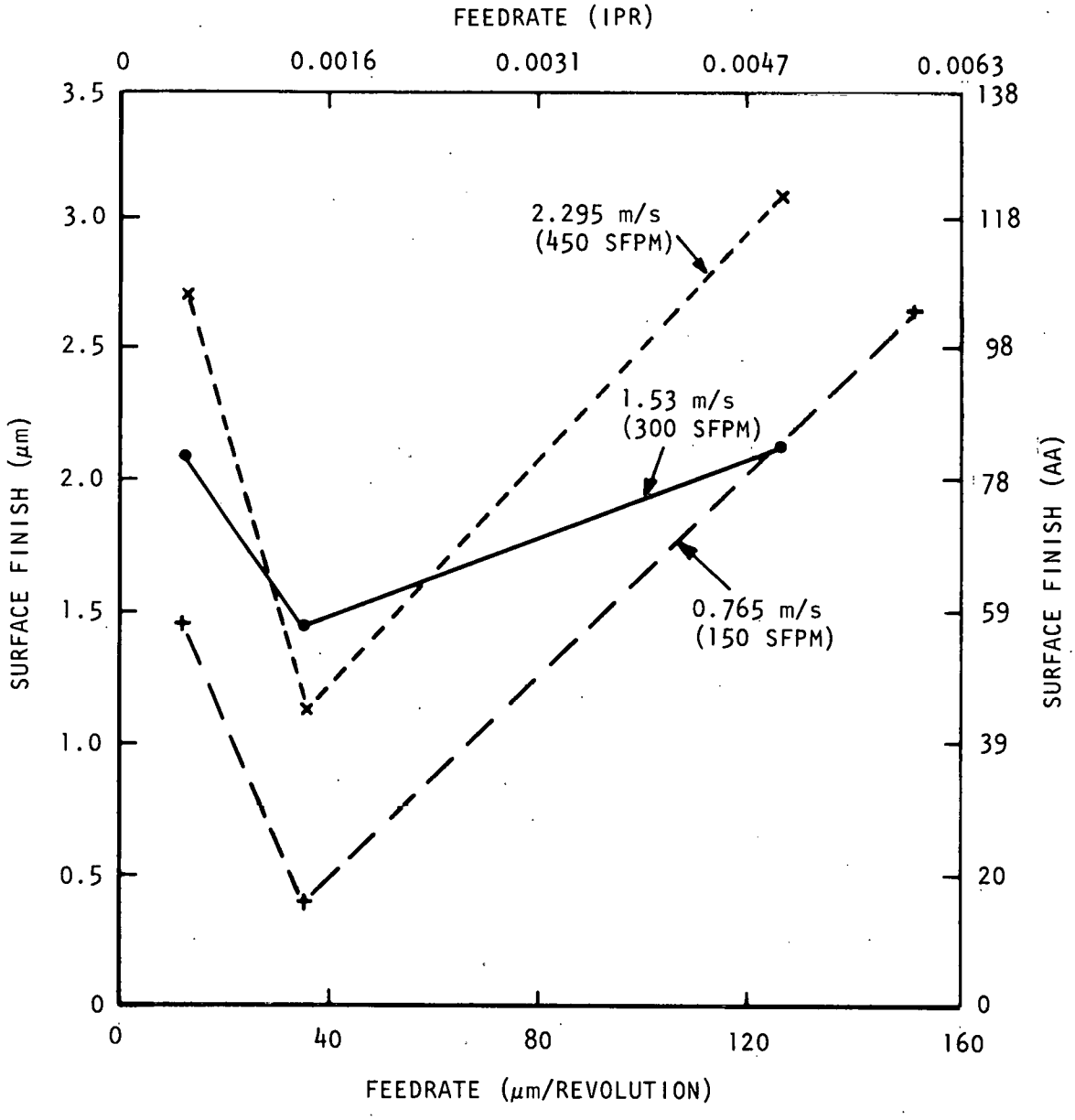

Figure 29. Effect of Feedrate and Spindle Speed on Surface Finish

The forces that were required to cut a workpiece from the bar stock also were monitored. Figure 30 shows the forces that were produced when a radial feedrate of 38.1 μm/revolution (0.0015 ipr) and a speed of 300 rpm were used. A 1.5-mm-wide (0.060 inch) tool, made from M2 HSS and having a 7-degree back rake, a 10-degree ECEA, a 1-degree side clearance, and a 15-degree end clearance, was used (BKC Tool 190367-031).

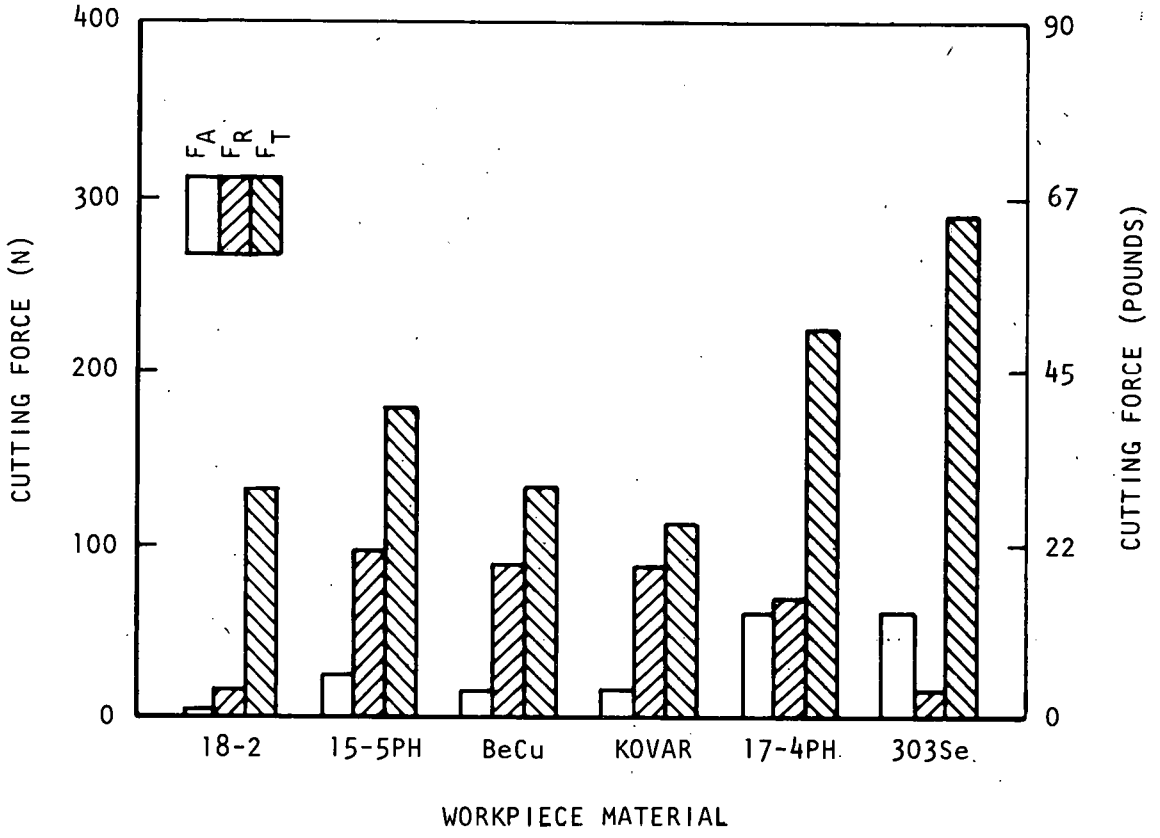

Figure 30. Cutting Forces on 1.5-mm-Wide (0.060 Inch) Cutoff Tool

The fact is significant that a tool which is only 1.5 mm wide can easily generate forces of 13.6 kg (30 pounds); these forces can create large deflections when small-diameter stock is used.

Production Implications

The studies described in this report were performed on stock that is larger than that which normally is used for the production of miniature precision parts. This was done to accommodate the cutting-force instrumentation and to eliminate chatter. While workpiece properties vary with the stock size, the data here presented can be considered representative of that which are encountered in the production of small parts. Since the cutting forces are essentially independent of the stock size, workpiece deflection can be easily seen to be a major problem in producing small parts. From the cantilever-beam theory, a 1.52-mm-diameter (0.060 inch) rod 6.35 mm (0.250 inch) long will deflect according to the following equation when a force is applied to the end.

$$\Delta = \frac{64FL^3}{3E\pi D^4}, \qquad (27)$$

where

Δ = deflection,

F = applied force,

L = length of rod,

E = modulus of elasticity, and

D = rod diameter.

From Table 13, a deflection for 303Se stainless steel of 85.3 μm (0.0034 inch) could be expected to result in a tapered diameter and, in many cases, chatter. While feedrates, tool geometries, coolants, and other factors usually are adjusted to solve this problem, all possible techniques should be utilized to minimize the deflection of miniature precision parts; selecting and controlling the workpiece properties is one approach that often is overlooked. For many small parts, the available spindle speed is not high enough to obtain the optimum cutting velocity. The following generalizations concerning the production of miniature precision parts can be made.

- Maximum fillet radii of 50.8 μm (0.002 inch) can be produced in stainless steel having a hardness of R_C45, but the life of HSS tools is short: in the order of 15 minutes or 635 linear mm (25 inches) of cut. For most materials, a more realistic maximum-fillet-radius requirement would be 76.2 μm (0.003 inch).

- Surface finishes of 0.56 μm (22 microinches) AA can be produced with tools having a nose radius of 76.2 μm (0.003 inch) and fed at a rate of 36.6 μm/revolution (0.00144 ipr). A more typical surface-finish value, however, with the described nose radius and feedrate is 1.07 μm (42 microinches). A 2.0-degree ECEA produces noticeably better finishes than do larger clearance angles.

- Burr height increases dramatically as the strain-hardening exponent (n) increases. Thus materials with high strain-hardening exponents produce long burrs.

- Materials with high strain-hardening exponents produce thicker burrs than those with lower values of n.

- Feedrates below 36.6 μm/revolution (0.00144 ipr) greatly increase the cutting forces, particularly in strain-hardening materials.

- Conventional wearland definitions for the end of tool life are meaningless when the end of life is defined by the maximum fillet radius.

- Conventional tool geometries are close to the geometries that typically are found to be optimum for machining miniature precision parts.

- Typically, tools show a radial wear of 76.2 μm (0.003 inch) after completing 1.4 m (55 inches) of cut.

- A 127-μm (0.005 inch) depth-of-cut at a feedrate of 36.6 μm/revolution (0.00144 ipr) and a speed of 0.406 μm/s (80 sfpm) results in a cutting force of 44.48 to 88.96 N (10 to 20 pounds) in the metals studied.

One of the basic limitations of the regression equations that were established during this study is the fact that they were based on only a few data points. Equation 23, for example, required five materials in order to solve for the five variables. Because of the choice of the side rake and back rake angles used, only two basic values of AE result (10 or 5). Thus a great amount of confidence cannot be placed in the use of these equations for determining optimum values which would be useful in other situations.

Material Selection

Machinability, while a major consideration in the choice of any workpiece material, is not the only significant factor. The following characteristics are some of the other factors that also must be considered:

- Tensile strength;
- Ductility;
- Cost;
- Corrosion resistance;
- Electrical characteristics;
- Abrasion resistance;
- Fatigue resistance;

- Density; and
- Dimensional stability.

Dimensional Stability

A secondary objective of this study was to determine the dimensional stability of the stainless steels that typically are used at Bendix Kansas City. If a tolerance of ±5.08 μm (±0.0002 inch) cannot be held on a part because the heat from machining causes a subsequent growth or contraction, machinability and tool wear tests alone will not provide a true indication of producibility.

Dimensional changes occur as a result of heat-treating operations, thermal expansion, relaxation of residual stresses, gradual phase changes, or the presence of magnetic fields. Changes due to thermal expansion or magnetic fields typically are from 0.127 to 1.270 μm (5 to 50 microinches), and they can be closely predicted. Changes due to heat-treating can be predicted, but in the case of 17-4PH stainless steel, the results will vary somewhere within a range of 5.08 to 20.32 μm/μm (0.0002 to 0.0008 inch/inch). Parts thus must have 15.24-μm (0.0006 inch) tolerances just to accommodate possible heat-treatment-related variations.

Dimensional changes caused by the relaxation of residual stresses are difficult to predict because the machining conditions used and the workpiece shape and material affect the magnitude of the change and probably the stability of the stresses. The basic metallurgical structure of a material offers some clues to its relative stability. If the stability of the metallurgical phases in a metal are known, then the stability of the material is known. The mere knowledge of the number of phases that exist in the workpiece material offers a less-accurate but usable estimate of stability.

Materials that are composed of a single metallurgical phase generally are more stable than a similar metal having two phases. Phase changes usually involve changes in size. In a two-phase material such as 416 stainless steel, the retained austenite is slowly transformed into martensite. Temperature changes in 416 stainless steel result in phase changes as well as changes from the normal thermal expansion. A material such as 303Se stainless steel, however, is essentially a very stable single-phase material (austenite).

Steel manufacturers generally rate the stability of the stainless steels in the order shown in Table 16. In a ranking provided by O'Boyle,[18] however, 416 stainless steel is indicated to be more stable than 303Se stainless steel (Table 17). In the latter

Table 16. Dimensional Stability of Stainless Steels

Stainless Steel	Remarks
303Se	Very stable because it is a single-phase material.
15-5PH	May exhibit some dimensional change.
416	Very susceptible to temperature changes; the retained austenite is transformed with age.

case, the 416 stainless steel has been subjected to a five-stage machining and heat-treating cycle; in most production instances, only a single heat-treating follows the machining operation. O'Boyle's article presents an excellent discussion of and some recommendations for achieving dimensional stability. Additional data and discussion are presented by Maringer[19] and Holden.[20]

ACCOMPLISHMENTS

The effects of tool geometry and depth-of-cut have been evaluated with respect to the size of the burr produced, the resulting surface finish, the cutting forces, and the fillet radii. Five tool angles were evaluated in five materials; two depths-of-cut and two levels of each angle were considered. Comparisons were made with tool geometries that typically are recommended for these materials under different cutting conditions.

The dimensional stability of each material also was briefly considered. Materials were ranked by their machinability, with machinability defined by burr size, surface finish, cutting forces, and fillet radius.

The use of conventional machinability rankings has been shown to be unrealistic for the manufacture of miniature precision parts.

FUTURE WORK

Although no future work is planned on this subject, a similar study performed on screw machines for parts having diameters less than 1.5 mm (0.060 inch) would be useful and more applicable to new components.

Table 17. Properties of Metals Used for Parts Requiring Good Dimensional Stability (O'Boyle)[18]

Metal	Stability Rating	Thermal Expansion (μin./in. or μm/m)	Coefficient of Thermal Expansion	
			μm/m/°C	μin./in./°F
2024-T4 Aluminum	Good	5	21.6	12.0
Graph-Mo Steel	Good	5	10.3	5.7
Ti-6 Al-4V	Good	5	8.6	4.8
416 Stainless Steel	Good	5	10.3	5.7
52100 Steel	Good	5	11.9	6.6
Gyromet	Good	5	5.9	3.3
Inconel	Fair	10	12.8	7.1
303Se Stainless Steel	Fair	10	16.0	8.9
304 Stainless Steel	Fair	10	16.0	8.9
Mallory 1000	Fair	10	5.4	3.0
7075-T6 Aluminum	Fair	10	23.4	13.0
356 Cast Aluminum	Poor	20	20.7	11.5
Cast Magnesium	Poor	200	25.2	14.0

REFERENCES

[1]L. K. Gillespie, "Machinability as Related to Precision Miniature Parts," SME Paper MRR-76-09, 1976.

[2]Deleted.

[3]G. F. Micheletti, "Work on Machinability in the Co-Operative Group C of CIRP and Outside This Group," *Annals of the CIRP*, Volume XVIII, 1970, pp 13-30.

[4]D. W. Davies, "Machinability: A Review of Criteria for Assessing Workpiece Materials in Small-Scale Drilling and Turning Tests," *Metallurgical Reviews*, Volume 13, 1967, p 41.

[5]Noel R. Parsons, editor, *N/C Machinability Data Systems*, SME, Dearborn, Michigan: 1971, p 80.

[6]Metcut Research Associates, Inc., *Machining Data Handbook*, 2nd edition. Cincinnati, Ohio: 1971.

[7]L. K. Gillespie, *Machining Miniature Slots and Fillets* (Final Report). UNCLASSIFIED. Bendix Kansas City: BDX-613-576, January, 1972 (Available from NTIS).

[8]Milton C. Shaw, *Metal Cutting Principles*, Cambridge, Massachusetts: Massachusetts Institute of Technology, 1954.

[9]G. Lorenz, "Composition and the Technological Properties of Free Cutting Brass," *Microtecnic*, Number 1, 1975, pp 45-49.

[10]M. C. Shaw and J. A. Crowell, "Finish Machining," *C.I.R.P. Annals*, Volume 13, 1965, pp 5-22.

[11]St. Enache, "Researches Concerning Optimum Geometry of the Finishing Tools with Nose Radius," *C.I.R.P. Annals*, Volume 16, 1971, pp 411-416.

[12]L. K. Gillespie, *The Formation and Properties of Machining Burrs*, MS Thesis, Utah State University, Logan, Utah, 1973.

[13]*Machining Data Handbook*. Cincinnati, Ohio: Machinability Data Center, 1972.

[14]*Recommended Machining Data on Beryllium Copper*, Kawecki Berylco Industries, Inc.

[15]*Machining Nickel Alloys*, brochure by International Nickel Company.

[16]F. J. McGee and others, "Optimum Cutter Geometry," *American Machinist*, September 22, 1969, pp 99-106.

[17]F. J. McGee, "How to Determine Tool Geometries for Optimum Performance," *Cutting Tool Engineering*, December, 1966, pp 15-21.

[18]Dennis O'Boyle, "How to Improve Dimensional Stability in Precision Metal Parts," *Machine Design*, January 30, 1964, pp 113-117.

[19]R. G. Maringer, *Review of Dimensional Instability in Metals*, Defense Metals Information Center Memorandum 213, June 23, 1966 (Available from NTIS under Accession Number 487419).

[20]F. C. Holden, *A Review of Dimensional Instability in Metals*, Defense Metals Information Center Memorandum 189, March 19, 1964 (Available from NTIS under Accession Number 602379).

Appendix

DATA TABLES

Table A-1. Workpiece-Material Properties

Property	Material					
	Kovar	Hiperco	15-5PH	303Se	BeCu	18-2
Yield Strength						
MPa	344.7	390.9	1034.1	413.6	654.9	576.6
KSI	50.0	56.7	150.0	60.0	95.0	83.5
Tensile Strength						
MPa	723.2	390.9	1137.5	551.5	703.2	625.3
KSI	104.9	56.7	165.0	80.0	102.0	90.7
Elongation in 50.8 mm or 2 Inches (Percent)	71.5	0.78	16.0	50.0	26.0	16.0
Reduction of Area (Percent)		0	58.0	55.0		48.0
Hardness (Brinell 3000 kg)	176	290	352	160	216	230
Strain-Hardening Exponent	0.42	0	0.08	0.56	0.10	0.12
Modulus of Elasticity						
GPa	137.90	206.82	199.93	199.93	127.54	193.03
PSI x 10^6	20.0	30.0	29.0	29.0	18.5	28.0

Table A-2. Values of W_N

Factor Levels	W_N for Indicated Material* ($W/cm^3/s$; $HP/in.^3/min$)					
	303Se	15-5PH	BeCu	Kovar	Hiperco	18-2
111111	2.66 (3.507)	1.73 (2.280)	0.80 (1.052)	1.46 (1.929)	2.53 (3.332)	2.26 (2.981)
111221	4.66 (6.138)	2.18 (2.876)	1.06 (1.403)	1.78 (2.350)	2.85 (3.753)	1.33 (1.754)
112112	7.32 (9.645)	2.40 (3.157)	1.60 (2.104)	2.66 (3.507)	6.26 (8.242)	1.33 (1.754)
112222	3.73 (4.910)	2.66 (3.507)	1.33 (1.754)	2.13 (2.806)	2.66 (3.507)	1.86 (2.455)
121122	3.19 (4.209)	2.66 (3.507)	1.20 (1.578)	1.86 (2.455)	3.33 (4.384)	1.86 (2.455)
121212	4.92 (6.488)	2.53 (3.332)	1.60 (2.104)	2.66 (3.507)	3.59 (4.735)	1.86 (2.455)
122121	4.45 (5.857)	2.00 (2.630)	0.88 (1.157)	1.60 (2.104)	2.80 (3.683)	1.33 (1.754)
122211	3.41 (4.489)	2.00 (2.630)	0.88 (1.157)	1.52 (1.999)	2.53 (3.332)	0.56 (0.737)
211122	3.99 (5.261)	3.99 (5.261)	1.33 (1.754)	1.86 (2.455)	6.26 (8.242)	1.46 (1.929)
211212	3.19 (4.209)	2.66 (3.507)	1.33 (1.754)	1.33 (1.754)	4.26 (5.612)	1.86 (2.455)
212121	2.77 (3.648)	1.73 (2.280)	0.80 (1.052)	1.60 (2.104)	2.66 (3.507)	1.60 (2.104)
212211	4.53 (5.962)	2.40 (3.157)	1.06 (1.403)	1.73 (2.280)	3.46 (4.559)	1.65 (2.175)

Table A-2 Continued. Values of W_N

Factor Levels	W_N for Indicated Material* ($W/cm^3/s$; $Hp/in.^3/min$)					
	303Se	15-5PH	BeCu	Kovar	Hiperco	18-2
221111	2.66 (3.507	2.05 (2.701)	1.04 (1.368)	1.86 (2.455)	3.06 (4.033)	1.60 (2.104)
221221	3.73 (4.910)	2.13 (2.806)	0.99 (1.298)	1.73 (2.280)	2.80 (3.683)	1.65 (2.175)
222112	5.32 (7.015)	2.66 (3.507)	2.00 (2.630)	2.13 (2.806)	2.93 (3.858)	1.73 (2.280)
222222	4.53 (5.962)	2.66 (3.507)	1.33 (1.754)	2.00 (2.630)	4.69 (6.138)	1.33 (1.754)

*Data is an average from two specimens at each of the indicated levels. See Table 3 in text for explanation of coding.

Table A-3. Average Surface-Finish Measurements

Factor Levels	Average Surface Finish for Indicated Material (μm; μin.)					
	303Se	15-5PH	BeCu	Kovar	Hiperco	18-2
111111	2.08 (82)	0.76 (30)	0.81 (32)	0.99 (39)	0.41 (16)	1.40 (55)
111221	1.19 (47)	0.79 (31)	0.86 (34)	0.91 (36)	0.41 (16)	1.09 (43)
112112	1.07 (42)	0.53 (21)	0.79 (31)	0.97 (38)	0.30 (12)	1.07 (42)
112222	1.37 (54)	0.41 (16)	1.35 (53)	1.30 (51)	0.38 (15)	1.35 (53)
121122	1.47 (58)	0.58 (23)	1.22 (48)	1.40 (55)	0.30 (12)	1.22 (48)
121212	1.02 (40)	1.88 (74)	1.02 (40)	1.32 (52)	0.46 (18)	1.52 (60)
122121	0.56 (22)	0.48 (19)	0.81 (32)	0.94 (37)	0.41 (16)	1.02 (40)
122211	1.22 (48)	0.81 (32)	1.14 (45)	1.40 (55)	1.12 (44)	1.14 (45)
211122	0.43 (17)	0.41 (16)	0.79 (31)	1.07 (42)	0.25 (10)	0.69 (27)
211212	0.64 (25)	0.15 (6)	1.07 (42)	0.97 (38)	0.25 (10)	2.24 (88)
212121	0.64 (25)	0.38 (15)	0.66 (26)	0.91 (36)	0.36 (14)	1.12 (44)
212211	0.33 (13)	0.56 (22)	0.71 (28)	1.02 (40)	0.20 (8)	1.12 (44)

Table A-3 Continued. Average Surface-Finish Measurements

Factor Levels	Average Surface Finish for Indicated Material (μm; μin.)					
	303Se	15-5PH	BeCu	Kovar	Hiperco	18-2
221111	0.28 (11)	0.41 (16)	0.91 (36)	0.97 (38)	0.18 (7)	1.12 (44)
221221	0.71 (28)	0.43 (17)	1.02 (40)	1.14 (45)	0.48 (19)	0.81 (32)
222112	0.25 (10)	0.51 (20)	0.36 (14)	1.45 (57)	0.25 (10)	2.41 (95)
222222	0.76 (30)	0.30 (12)	0.79 (31)	0.97 (38)	0.46 (18)	1.07 (42)

Table A-4. Average Burr Height

Factor Levels	Average Burr Height for Indicated Material (μm; In. x 10^{-4})					
	303Se	15-5PH	BeCu	Kovar	Hiperco	18-2
111111	277 (109)	20 (8)	41 (16)	46 (18)	56 (22)	20 (8)
111221	457 (180)	61 (24)	25 (10)	61 (24)	51 (20)	46 (18)
112112	493 (194)	20 (8)	25 (10)	86 (34)	117 (46)	48 (19)
112222	345 (136)	0 (0)	30 (12)	71 (28)	28 (11)	28 (11)
121122	241 (96)	0 (0)	15 (6)	46 (18)	36 (14)	33 (13)
121212	325 (128)	51 (20)	66 (26)	127 (50)	145 (57)	61 (24)
122121	366 (144)	30 (12)	48 (19)	91 (36)	43 (17)	25 (10)
122211	635 (250)	71 (28)	18 (7)	56 (22)	61 (24)	25 (10)
111122	485 (191)	20 (8)	66 (26)	76 (30)	61 (24)	56 (22)
211212	833 (328)	71 (28)	38 (15)	36 (14)	118 (44)	114 (45)
212121	450 (177)	0 (0)	30 (12)	64 (25)	48 (19)	38 (15)
212211	790 (311)	122 (48)	10 (4)	66 (26)	41 (16)	41 (16)

Table A-4 Continued. Average Burr Height

Factor Levels	Average Burr Height for Indicated Material (μm; In. x 10^{-4})					
	303Se	15-5PH	BeCu	Kovar	Hiperco	18-2
221111	544 (214)	41 (16)	25 (10)	46 (18)	109 (43)	41 (16)
221221	345 (136)	15 (6)	23 (9)	99 (39)	51 (20)	46 (18)
222112	254 (100)	41 (16)	30 (12)	142 (56)	0 (0)	30 (12)
222222	533 (210)	23 (9)	66 (26)	74 (29)	94 (37)	20 (8)

Table A-5. Average Burr Thickness

Factor Levels	Average Burr Thickness for Indicated Material (μm; In. x 10^{-4})					
	303Se	15-5PH	BeCu	Kovar	Hiperco	18-2
111111	124 (49)	51 (20)	76 (30)	79 (31)	91 (36)	46 (18)
111221	147 (58)	81 (32)	46 (18)	81 (32)	56 (22)	46 (18)
112112	152 (60)	20 (8)	33 (13)	81 (32)	97 (38)	61 (24)
112222	145 (57)	0 (0)	76 (30)	91 (36)	61 (24)	43 (17)
121122	97 (38)	0 (0)	30 (12)	66 (26)	33 (13)	33 (13)
121212	107 (42)	18 (7)	71 (28)	56 (22)	109 (43)	46 (18)
122121	246 (97)	36 (14)	56 (22)	46 (18)	66 (26)	41 (16)
122211	91 (36)	97 (38)	33 (13)	117 (46)	89 (35)	61 (24)
211122	833 (328)	18 (7)	20 (8)	61 (24)	30 (12)	36 (14)
211212	132 (52)	94 (37)	56 (22)	86 (34)	109 (43)	97 (38)
212121	124 (49)	0 (0)	61 (24)	76 (30)	71 (28)	20 (8)
212211	330 (130)	79 (31)	20 (8)	51 (20)	58 (23)	64 (25)

Table A-5 Continued. Average Burr Thickness

Factor Levels	Average Burr Thickness for Indicated Material (μm; In. x 10^{-4})					
	303Se	15-5PH	BeCu	Kovar	Hiperco	18-2
221111	935 (368)	64 (25)	20 (8)	69 (27)	76 (30)	33 (13)
221221	107 (42)	56 (22)	66 (26)	97 (38)	79 (31)	64 (25)
222112	86 (34)	61 (24)	58 (23)	89 (35)	0 (0)	56 (22)
222222	218 (86)	15 (6)	28 (11)	48 (19)	64 (25)	56 (22)

Table A-6. Average Fillet Radius

Factor Levels	Average Fillet Radius for Indicated Material (μm; In. x 10^{-4})					
	303Se	15-5PH	BeCu	Kovar	Hiperco	18-2
111111	61 (24)	41 (16)	107 (42)	58 (23)	137 (54)	117 (46)
111221	71 (28)	76 (30)	41 (16)	51 (20)	127 (50)	51 (20)
112112	66 (26)	46 (18)	41 (16)	61 (24)	97 (38)	46 (18)
112222	53 (21)	20 (8)	56 (22)	36 (14)	64 (25)	38 (15)
121122	36 (14)	53 (21)	48 (19)	58 (23)	56 (22)	36 (14)
121212	41 (16)	43 (17)	61 (24)	41 (16)	56 (22)	36 (14)
122121	147 (58)	51 (20)	157 (62)	86 (34)	114 (45)	86 (34)
122211	38 (15)	66 (26)	130 (51)	97 (38)	132 (52)	41 (16)
211122	36 (14)	78 (11)	53 (21)	38 (15)	76 (30)	41 (16)
211212	46 (18)	81 (32)	56 (22)	66 (26)	81 (32)	71 (28)
212121	53 (21)	107 (42)	51 (20)	69 (27)	155 (61)	51 (20)
212211	251 (99)	71 (28)	81 (32)	66 (26)	137 (54)	41 (16)

Table A-6 Continued. Average Fillet Radius

Factor Levels	Average Fillet Radius for Indicated Material (μm; In. x 10^{-4})					
	303Se	15-5PH	BeCu	Kovar	Hiperco	18-2
221111	30 (12)	36 (14)	61 (24)	30 (12)	114 (45)	61 (24)
221221	41 (16)	119 (47)	89 (35)	86 (34)	107 (42)	25 (10)
222112	43 (17)	64 (24)	56 (22)	64 (25)	25 (10)	36 (14)
222222	81 (32)	18 (7)	46 (18)	51 (20)	84 (33)	41 (16)

Table A-7. Average Cutting Force F_R

Factor Levels	Average Cutting Force F_R for Indicated Material (N; Pounds)					
	303Se	15-5PH	BeCu	Kovar	Hiperco	18-2
111111	35.6 (8)	0 (0)	-8.9 (-2)	-8.9 (-2)	0 (0)	17.8 (4)
111221	35.6 (8)	-17.8 (-4)	8.9 (2)	8.9 (2)	35.6 (8)	17.8 (4)
112112	0 (0)	0 (0)	4.4 (1)	4.4 (1)	22.2 (5)	4.4 (1)
112222	17.8 (4)	17.8 (4)	8.9 (2)	8.9 (2)	8.9 (2)	8.9 (2)
121122	17.8 (4)	8.9 (2)	8.9 (2)	8.9 (2)	13.3 (3)	4.4 (1)
121212	0 (0)	8.9 (2)	4.4 (1)	0 (0)	8.9 (2)	4.4 (1)
122121	40.0 (9)	-17.8 (-4)	8.9 (2)	8.9 (2)	17.8 (4)	17.8 (4)
122211	53.4 (12)	-53.4 (-12)	0 (0)	-8.9 (-2)	-26.7 (-6)	8.9 (2)
211122	0 (0)	17.8 (4)	4.4 (1)	4.4 (1)	17.8 (4)	4.4 (1)
211212	17.8 (4)	8.9 (2)	4.4 (1)	8.9 (2)	26.7 (6)	0 (0)
212121	35.6 (8)	26.7 (6)	-8.9 (-2)	-4.4 (-1)	44.8 (10)	8.9 (2)
212211	17.8 (4)	17.8 (4)	8.9 (2)	8.9 (2)	8.9 (2)	17.8 (4)

Table A-7 Continued. Average Cutting Force F_R

Factor Levels	Average Cutting Force F_R for Indicated Material (N; Pounds)					
	303Se	15-5PH	BeCu	Kovar	Hiperco	18-2
221111	17.8 (4)	31.1 (7)	8.9 (2)	17.8 (4)	13.3 (3)	8.9 (2)
221221	35.6 (8)	-17.8 (-4)	8.9 (2)	0 (0)	-4.4 (-1)	17.8 (4)
222112	48.9 (11)	17.8 (4)	17.8 (4)	8.9 (2)	13.3 (3)	4.4 (1)
222222	8.9 (2)	8.9 (2)	4.4 (1)	4.4 (1)	13.3 (3)	4.4 (1)

Table A-8. Average Cutting Force F_T

Factor Levels	Tool Number	Average Cutting Force F_T for Indicated Material (N; Pounds)					
		303Se	15-5PH	BeCu	Kovar	Hiperco	18-2
111111	1	222.4 (50)	142.3 (32)	66.7 (15)	124.5 (28)	213.5 (48)	186.8 (42)
111221	16	391.4 (88)	182.4 (41)	89.0 (20)	151.2 (34)	240.2 (54)	111.2 (25)
112112	15	124.5 (28)	40.0 (9)	26.7 (6)	44.5 (10)	106.8 (24)	22.2 (5)
112222	2	62.3 (14)	44.5 (10)	22.2 (5)	35.6 (8)	44.5 (10)	31.1 (7)
121122	3	53.4 (12)	44.5 (10)	17.8 (4)	31.1 (7)	53.4 (12)	31.1 (7)
121212	14	80.1 (18)	44.5 (10)	26.7 (6)	44.5 (10)	62.3 (14)	31.1 (7)
122121	13	373.6 (84)	169.0 (38)	71.2 (16)	133.4 (30)	231.3 (52)	111.2 (25)
122211	4	284.7 (64)	169.0 (38)	71.2 (16)	124.5 (28)	213.5 (48)	44.5 (10)
211122	12	66.7 (15)	66.7 (15)	22.2 (5)	31.1 (7)	106.8 (24)	26.7 (6)
211212	5	53.4 (12)	44.5 (10)	22.2 (5)	40.0 (9)	71.2 (16)	31.1 (7)
212121	6	231.3 (52)	142.3 (32)	66.7 (15)	133.4 (30)	222.4 (50)	133.4 (30)
212211	11	378.1 (85)	200.3 (45)	89.0 (20)	142.3 (32)	289.1 (65)	137.9 (31)

Table A-8 Continued. Average Cutting Force F_T

Factor Levels	Tool Number	Average Cutting Force F_T for Indicated Material (N; Pounds)					
		303Se	15-5PH	BeCu	Kovar	Hiperco	18-2
221111	10	222.4 (50)	169.0 (38)	89.0 (20)	155.7 (35)	258.0 (58)	133.4 (30)
221221	7	311.4 (70)	177.9 (40)	80.1 (18)	142.3 (32)	231.3 (52)	137.9 (31)
222112	8	89.0 (20)	44.5 (10)	35.6 (8)	35.6 (8)	48.9 (11)	26.7 (6)
222222	9	75.6 (17)	44.5 (10)	22.2 (5)	35.6 (8)	80.1 (18)	22.2 (5)

Table A-9. Average Cutting Force F_A

Factor Levels	Average Cutting Force F_A for Indicated Material (N; Pounds)					
	303Se	15-5PH	BeCu	Kovar	Hiperco	18-2
111111	142.3 (32)	75.6 (17)	17.8 (4)	53.4 (12)	115.6 (26)	35.6 (8)
111221	173.5 (39)	80.1 (18)	35.6 (8)	53.4 (12)	89.0 (20)	44.5 (10)
112112	35.6 (8)	8.9 (2)	8.9 (2)	17.8 (4)	17.8 (4)	8.9 (2)
112222	22.2 (5)	17.8 (4)	8.9 (2)	17.8 (4)	22.2 (5)	8.9 (2)
121122	22.2 (5)	17.8 (4)	8.9 (2)	17.8 (4)	26.7 (6)	8.9 (2)
121212	35.6 (8)	17.8 (4)	8.9 (2)	17.8 (4)	26.7 (6)	8.9 (2)
122121	155.7 (35)	62.3 (14)	26.7 (6)	44.5 (10)	80.1 (18)	31.1 (7)
122211	177.9 (40)	80.1 (18)	35.6 (8)	71.2 (16)	115.6 (26)	35.6 (8)
211122	35.6 (8)	13.3 (3)	8.9 (2)	13.3 (3)	17.8 (4)	8.9 (2)
211212	44.5 (10)	17.8 (4)	8.9 (2)	26.7 (6)	26.7 (6)	8.9 (2)
212121	155.7 (35)	71.2 (16)	26.7 (6)	53.4 (12)	111.2 (25)	35.6 (8)
212211	177.9 (40)	80.1 (18)	26.7 (6)	62.3 (14)	97.9 (22)	48.9 (11)

Table A-9 Continued. Average Cutting Force F_A

Factor Levels	Average Cutting Force F_A for Indicated Material (N; Pounds)					
	303Se	15-5PH	BeCu	Kovar	Hiperco	18-2
221111	89.0 (20)	80.1 (18)	26.7 (6)	62.3 (14)	89.0 (20)	44.5 (10)
221221	177.9 (40)	89.0 (20)	35.6 (8)	71.2 (16)	129.0 (29)	44.5 (10)
222112	35.6 (8)	17.8 (4)	8.9 (2)	17.8 (4)	22.2 (5)	8.9 (2)
222222	89.0 (20)	17.8 (4)	8.9 (2)	17.8 (4)	17.8 (4)	8.9 (2)

Table A-10. Average Localized Wearland Thickness C*

Factor Levels	Average Thickness for Indicated Material (μm; mils)					
	303Se	15-5PH	BeCu	Kovar	Hiperco	18-2
111221	177.8 (7.0)	63.5 (2.5)	12.7 (0.5)	0 (0)	203.2 (8.0)	0 (0)
112112	20.3 (0.8)	50.8 (2.0)	50.8 (2.0)	0 (0)	88.9 (3.5)	25.4 (1.0)
121212	25.4 (1.0)	25.4 (1.0)	63.5 (2.5)	12.7 (0.5)	25.4 (1.0)	12.7 (0.5)
122121	165.1 (6.5)	88.9 (3.5)	12.7 (0.5)	0 (0)	203.2 (8.0)	0 (0)
211122	38.1 (1.5)	25.4 (1.0)	12.7 (0.5)	25.4 (1.0)	38.1 (1.5)	0 (0)
212211	88.9 (3.5)	76.2 (3.0)	25.4 (1.0)	0 (0)	279.4 (11.0)	0 (0)
221111	88.9 (3.5)	63.5 (2.5)	177.8 (7.0)	0 (0)	241.3 (9.5)	50.8 (2.0)
222222	50.8 (2.0)	0 (0)	25.4 (1.0)	25.4 (1.0)	38.1 (1.5)	0 (0)

*Refer to Figure 22 for definition of wearland position.

Table A-11. Average Localized Wearland Thickness B*

Factor Levels	Average Thickness for Indicated Material (μm; mils)					
	303Se	15-5PH	BeCu	Kovar	Hiperco	18-2
111221	139.7 (5.5)	63.5 (2.5)	38.1 (1.5)	38.1 (1.5)	190.5 (7.5)	0 (0)
112112	76.2 (3.0)	127.0 (5.0)	63.5 (2.5)	25.4 (1.0)	317.5 (12.5)	0 (0)
121212	76.2 (3.0)	114.3 (4.5)	88.9 (3.5)	50.8 (2.0)	203.2 (8.0)	0 (0)
122121	127.0 (5.0)	88.9 (3.5)	50.8 (2.0)	76.2 (3.0)	190.5 (7.5)	0 (0)
211122	76.2 (3.0)	152.4 (6.0)	63.5 (2.5)	50.8 (2.0)	254.0 (10.0)	0 (0)
212211	127.0 (5.0)	76.2 (3.0)	50.8 (2.0)	25.4 (1.0)	279.4 (11.0)	0 (0)
221111	190.5 (7.5)	88.9 (3.5)	25.4 (1.0)	50.8 (2.0)	228.6 (9.0)	177.8 (7.0)
222222	165.1 (6.5)	114.3 (4.5)	50.8 (2.0)	50.8 (2.0)	203.2 (8.0)	0 (0)

*Refer to Figure 22 for definition of wearland position.

Table A-12. Average Localized Wearland Thickness A*

Factor Levels	Average Thickness for Indicated Material (μm; mils)					
	303Se	15-5PH	BeCu	Kovar	Hiperco	18-2
111221	317.5 (12.5)	254.0 (10.0)	114.3 (4.5)	114.3 (4.5)	393.7 (15.5)	101.6 (4.0)
112112	152.4 (6.0)	177.8 (7.0)	152.4 (6.0)	127.0 (5.0)	546.1 (21.5)	114.3 (4.5)
121212	127.0 (5.0)	203.2 (8.0)	254.0 (10.0)	101.6 (4.0)	381.0 (15.0)	203.2 (8.0)
122121	292.1 (11.5)	177.8 (7.0)	228.6 (9.0)	139.7 (5.5)	393.7 (15.5)	25.4 (1.0)
211122	127.0 (5.0)	279.4 (11.0)	190.5 (7.5)	114.3 (4.5)	469.9 (18.5)	50.8 (2.0)
212211	330.2 (13.0)	177.8 (7.0)	165.1 (6.5)	101.6 (4.0)	533.4 (21.0)	50.8 (2.0)
221111	76.2 (3.0)	254.0 (10.0)	165.1 (6.5)	101.6 (4.0)	508.0 (20.0)	279.4 (11.0)
222222	101.6 (4.0)	152.4 (6.0)	114.3 (4.5)	101.6 (4.0)	355.6 (14.0)	20.3 (0.8)

*Refer to Figure 22 for definition of wearland position.

Table A-13. Tool-Angle Combinations Producing Lowest and Highest Cutting Force F_T

Cutting Force F_T	Variable Angle	Tool Angles for Indicated Material* (Degrees)					
		303Se	15-5PH	BeCu	Kovar	Hiperco	18-2
Lowest							
	ECEA	7, 7	7, 2	7, 7	7, 7	7, 7	7, 7
	SR	10, 10	10, 5	10, 5	10, 5	10, 5	5, 5
	BR	5, 0	5, 5	5, 0	5, 0	5, 0	0, 5
Highest							
	ECEA	7, 7	2, 2	7, 2	7, 2	2, 2	7, 2
	SR	5, 10	10, 5	0, 5	5, 10	10, 5	10, 5
	BR	5, 0	5, 0	0, 0	5, 5	5, 0	5, 0

*The geometry of the two tools producing the lowest force and the highest force are given.

Table A-14. ANOVA Summary for F_T

Defects	Material					
	303Se	15-5PH	BeCu	Kovar	Hiperco	18-2
ECEA (A)					**	
ERf (B)					*	*
BR (C)	*					*
SR (D)	*	*				*
SCEA (E) [ABD]****						
Depth-Of-Cut (F) [ABC]	***	***	***	***	***	***
ECEA x ERf (AB)			*			*
ECEA x BR (AC)						*
ECEA x SR (AD)						*
ERf x BR (BC)				*		
ERf x SR (BD)	*	*	**			
BR x SR (CD)	**					
ECEA x BR x SR (ACD)	**	**	**	*	**	
ERf x BR x SR (BCD)						*
ECEA x ERf x BR x SR (ABCD)	**	**	**		*	*

*Significant effect at 95-percent confidence level.
**Significant effect at 99-percent confidence level.
***Significant effect at a confidence level exceeding 99 percent.
****[]Equated to the factor to generate the fractional replicate.

Table A-15. ANOVA Summary for F_A

	Material					
Defects	303Se	15-5PH	BeCu	Kovar	Hiperco	18-2
ECEA (A)	*			***		**
ERf (B)			*	**		
BR (C)	***			*	*	*
SR (D)	***	**	***	***	**	**
SCEA (E) [ABD]****	***		*	***		*
Depth-Of-Cut (F) [ABC]	***	***	***	***	***	***
ECEA x ERf (AB)	**					
ECEA x BR (AC)	***		*	***		
ECEA x SR (AD)	***					
ERf x BR (BC)	***				*	*
ERf x SR (BD)	***			*	**	
BR x SR (CD)	**		**	*		
ECEA x BR x SR (ACD)				***	***	
ERf x BR x SR (BCD)				*		
ECEA x ERf x BR x SR (ABCD)	***		**	***		*

*Significant effect at 95-percent confidence level.
**Significant effect at 99-percent confidence level.
***Significant effect at a confidence level exceeding 99 percent.
****[]Equated to the factor to generate the fractional replicate.

Table A-16. ANOVA Summary for F_R

Defects	Material					
	303Se	15-5PH	BeCu	Kovar	Hiperco	18-2
ECEA (A)		***		***	*	*
ERf (B)	*	**	**	*	**	
BR (C)	*					
SR (D)		**			**	
SCEA (E) [ABD]****					**	
Depth-Of-Cut (F) [ABC]	***	***	**	***		***
ECEA x ERf (AB)				*		
ECEA x BR (AC)		**	*	**	*	
ECEA x SR (AD)						
ERf x BR (BC)	**	***		**		
ERf x SR (BD)		**	***	***	*	
BR x SR (CD)					**	
ECEA x BR x SR (ACD)	***		*	***	*	
ERf x BR x SR (BCD)			*		*	
ECEA x ERf x BR x SR (ABCD)		***	**		*	*

*Significant effect at 95-percent confidence level.
**Significant effect at 99-percent confidence level.
***Significant effect at a confidence level exceeding 99 percent.
****[]Equated to the factor to generate the fractional replicate.

Table A-17. ANOVA Summary for Fillet Radius

Defects	Material					
	303Se	15-5PH	BeCu	Kovar	Hiperco	18-2
ECEA (A)						
ERf (B)						
BR (C)	**					
SR (D)						
SCEA (E) [ABD]****						
Depth-Of-Cut (F) [ABC]	**	**	**	**	**	
ECEA x ERf (AB)	*					
ECEA x BR (AC)						
ECEA x SR (AD)	**			*		
ERf x BR (BC)						
ERf x SR (BD)	*					
BR x SR (CD)		**				
ECEA x BR x SR (ACD)	**	*		*		
ERf x BR x SR (BCD)	*		*			
ECEA x ERf x BR x SR (ABCD)						

*Significant effect at 95-percent confidence level.
**Significant effect at 99-percent confidence level.
***Significant effect at a confidence level exceeding 99 percent.
****[]Equated to the factor to generate the fractional replicate.

Table A-18. ANOVA Summary for Surface Finish

Defects	Material					
	303Se	15-5PH	BeCu	Kovar	Hiperco	18-2
ECEA (A)	***	**	***	*		
ERf (B)	*	*		***		
BR (C)	*	*	**			
SR (D)			***			
SCEA (E) [ABD]****		**	*			**
Depth-Of-Cut (F) [ABC]				**		*
ECEA x ERf (AB)	*					
ECEA x BR (AC)	*	**	***			
ECEA x SR (AD)	*	**		**		
ERf x BR (BC)			**			
ERf x SR (BD)	**	*			*	*
BR x SR (CD)	**		**			*
ECEA x BR x SR (ACD)	**	*	**	***		**
ERf x BR x SR (BCD)		*		*		
ECEA x ERf x BR x SR (ABCD)			**			

*Significant effect at 95-percent confidence level.
**Significant effect at 99-percent confidence level.
***Significant effect at a confidence level exceeding 99 percent.
****[]Equated to the factor to generate the fractional replicate.

Table A-19. ANOVA Summary for Burr Height

Defects	Material					
	303Se	15-5PH	BeCu	Kovar	Hiperco	18-2
ECEA (A)				***		
ERf (B)				***		
BR (C)				***		**
SR (D)		**		***		
SCEA (E) [ABD]****		**		***	*	
Depth-Of-Cut (F) [ABC]				***		*
ECEA x ERf (AB)		*		***		*
ECEA x BR (AC)				***		
ECEA x SR (AD)				***		
ERf x BR (BC)				***		
ERf x SR (BD)		*		***	*	
BR x SR (CD)				***		*
ECEA x BR x SR (ACD)		*		***	*	
ERf x BR x SR (BCD)				***		
ECEA x ERf x BR x SR (ABCD)				***	*	

*Significant effect at 95-percent confidence level.
**Significant effect at 99-percent confidence level.
***Significant effect at a confidence level exceeding 99 percent.
****[ ]Equated to the factor to generate the fractional replicate.

Table A-20. ANOVA Summary for Burr Thickness

Defects	Material					
	303Se	15-5PH	BeCu	Kovar	Hiperco	18-2
ECEA (A)						
ERf (B)						
BR (C)						
SR (D)		*				*
SCEA (E) [ABD]****						*
Depth-Of-Cut (F) [ABC]		*				
ECEA x ERf (AB)						
ECEA x BR (AC)						
ECEA x SR (AD)						*
ERf x BR (BC)		*				
ERf x SR (BD)						
BR x SR (CD)						
ECEA x BR x SR (ACD)	*	**		**		
ERf x BR x SR (BCD)						
ECEA x ERf x BR x SR (ABCD)						

*Significant effect at 95-percent confidence level.
**Significant effect at 99-percent confidence level.
***Significant effect at a confidence level exceeding 99 percent.
****[]Equated to the factor to generate the fractional replicate.

Table A-21. Alias Structure for Design of Geometry-Effect Tests

Equivalents
I = ABDE = ABCF = CDEF
A = BDE = BCF = ACDEF
B = ADE = ACF = BCDEF
C = ABF = DEF = ABCDE
D = ABE = CEF = ABCDF
E = ABD = CDF = ABCEF
F = ABC = CDF = ABDEF
AB = CF = DE = ABCDEF
AC = BF = ADEF = BCDE
AD = BE = ACEF = BCDF
BC = AF = ACDE = BDEF
BD = AE = ACDE = BCEF
CD = EF = ABCE = ABDF
ACD = AEF = BCE = BDF
BCD = ACE = ADF = BEF
ABCD = CE = DF = ADEF

Table A-22. Wearland Heights for Tests Involving Only Two Specimens

Wearland Position	Tool	Factor Levels	Wearland Height for Indicated Material (μm; Inch) 303Se	15-5PH	Kovar	BeCu	Hiperco	18-2
A*	9	222222	101.6 (0.0040)	152.4 (0.0060)	114.3 (0.0045)	101.6 (0.0040)	355.6 (0.0140)	20.3 (0.0008)
	10	221111	76.2 (0.0030)	254.0 (0.0100)	165.1 (0.0065)	101.6 (0.0040)	508.0 (0.0200)	279.4 (0.0110)
	11	212211	330.2 (0.0130)	177.8 (0.0070)	165.1 (0.0065)	101.6 (0.0040)	533.4 (0.0210)	50.8 (0.0020)
	12	211122	127.0 (0.0050)	279.4 (0.0110)	444.5 (0.0175)	114.3 (0.0045)	469.9 (0.0185)	50.8 (0.0020)
	13	122121	292.1 (0.0115)	177.8 (0.0070)	228.6 (0.0090)	127.0 (0.0055)	393.7 (0.0155)	25.4 (0.0010)
	14	121212	127.0 (0.0050)	203.2 (0.0080)	254.0 (0.0100)	152.4 (0.0060)	381.0 (0.0150)	203.0 (0.0080)
	15	112112	152.4 (0.0060)	177.8 (0.0070)	152.4 (0.0060)	127.0 (0.0050)	546.1 (0.0215)	114.3 (0.0045)
	16	111221	317.5 (0.0125)	254.0 (0.0100)	114.3 (0.0045)	114.3 (0.0045)	393.7 (0.0155)	101.6 (0.0040)
	Avg.		190.5 (0.0075)	208.3 (0.0082)	205.7 (0.0081)	119.4 (0.0047)	447.0 (0.0176)	106.7 (0.0042)
B	9	222222	165.1 (0.0065)	114.3 (0.0045)	50.8 (0.0020)	50.8 (0.0020)	203.2 (0.0080)	**
	10	221111	177.8 (0.0075)	88.9 (0.0035)	25.4 (0.0010)	50.8 (0.0020)	381.0 (0.0150)	177.8 (0.0070)
	11	212211	127.0 (0.0050)	76.2 (0.0030)	50.8 (0.0020)	25.4 (0.0010)	406.4 (0.0160)	

Table A-22 Continued. Wearland Heights for Tests Involving Only Two Specimens

Wearland Position	Tool	Factor Levels	Wearland Height for Indicated Material (μm; Inch) 303Se	15-5PH	Kovar	BeCu	Hiperco	18-2
B	12	211122	76.2 (0.0030)	152.4 (0.0060)	63.5 (0.0025)	50.8 (0.0020)	254.0 (0.0100)	
	13	122121	127.0 (0.0050)	88.9 (0.0035)	50.8 (0.0020)	76.2 (0.0030)	304.8 (0.0120)	
	14	121212	76.2 (0.0030)	114.3 (0.0045)	88.9 (0.0035)	50.8 (0.0020)	203.2 (0.0080)	
	15	112112	76.2 (0.0030)	127.0 (0.0050)	63.5 (0.0025)	25.4 (0.0010)	304.8 (0.0120)	
	16	111221	139.7 (0.0055)	63.5 (0.0025)	38.1 (0.0015)	38.1 (0.0015)	304.8 (0.0120)	
	Avg.		101.6 (0.0048)	104.1 (0.0041)	53.3 (0.0021)	45.7 (0.0018)	294.6 (0.0116)	25.4 (0.0010)
C	9	222222	50.8 (0.0020)		25.4 (0.0010)	25.4 (0.0010)	38.1 (0.0015)	
	10	221111	88.9 (0.0035)	63.5 (0.0025)	17.8 (0.0007)	0 (0.0000)	241.3 (0.0095)	50.8 (0.0020)
	11	212211	88.9 (0.0035)	76.2 (0.0030)	25.4 (0.0010)		279.4 (0.0110)	
	12	211122	38.1 (0.0015)	25.4 (0.0010)	12.7 (0.0005)	25.4 (0.0010)	38.1 (0.0015)	
	13	122121	165.1 (0.0065)	88.9 (0.0035)	12.7 (0.0005)		203.2 (0.0080)	
	14	121212	25.4 (0.0010)	25.4 (0.0010)	63.5 (0.0025)	12.7 (0.0005)	25.4 (0.0010)	12.7 (0.0005)

Table A-22 Continued. Wearland Heights for Tests Involving Only Two Specimens

Wearland Position	Tool	Factor Levels	Wearland Height for Indicated Material (μm;Inch) 303Se	15-5PH	Kovar	BeCu	Hiperco	18-2
C	15	112112	20.3 (0.0008)	50.8 (0.0020)	50.8 (0.0020)		88.9 (0.0035)	25.4 (0.0010)
	16	111221	177.8 (0.0070)	63.5 (0.0025)	63.5 (0.0025)		203.2 (0.0080)	
	Avg.		81.3 (0.0032)	48.3 (0.0019)	33.0 (0.0013)	7.6 (0.0003)	139.7 (0.0055)	10.2 (0.0004)

*Refer to Figure 22 for definition of wearland positions.
**Blank spaces indicate that no measurements were made.

Table A-23. Constants for Tool-Wear Equations

Material	Factor Levels	Variable and Measuring Units	Constants* a_1	Constants* a_2
15-5PH	122211	$F_{A_{(N;\ Pounds)}}$	80.6 (18.13)	2.98 (0.67)
BeCu	211212	$F_{A_{(N;\ Pounds)}}$	8.9 (2.0)	1.1 (0.25)
Kovar	221221	$F_{A_{(N;\ Pounds)}}$	67.6 (15.2)	2.6 (0.58)
Kovar	222112	$F_{A_{(N;\ Pounds)}}$	16.3 (3.67)	0.7 (0.15)
Hiperco	111111	$F_{A_{(N;\ Pounds)}}$	114.5 (25.73)	4.3 (0.96)
Hiperco	121122	$F_{A_{(N;\ Pounds)}}$	21.7 (4.87)	2.1 (0.48)
Hiperco	221221	$F_{A_{(N;\ Pounds)}}$	125.7 (28.27)	2.8 (0.64)
Hiperco	222112	$F_{A_{(N;\ Pounds)}}$	20.1 (4.53)	0.9 (0.21)
BeCu	111111	$F_{T_{(N;\ Pounds)}}$	62.6 (14.07)	2.5 (0.57)
BeCu	112222	$F_{T_{(N;\ Pounds)}}$	20.1 (4.53)	0.8 (0.18)
Hiperco	111111	$F_{T_{(N;\ Pounds)}}$	208.5 (46.87)	12.4 (2.79)
Hiperco	112222	$F_{T_{(N;\ Pounds)}}$	36.2 (8.13)	6.7 (1.50)
Hiperco	211212	$F_{T_{(N;\ Pounds)}}$	71.5 (16.07)	12.7 (2.86)
Hiperco	212121	$F_{T_{(N;\ Pounds)}}$	216.5 (48.67)	11.6 (2.60)
Hiperco	221221	$F_{T_{(N;\ Pounds)}}$	223.9 (50.33)	8.2 (1.85)
Hiperco	222112	$F_{T_{(N;\ Pounds)}}$	45.4 (10.20)	7.4 (1.67)
303Se	221221	$F_{R_{(N;\ Pounds)}}$	35.6 (8.00)	2.3 (0.51)

Table A-23 Continued. Constants for Tool-Wear Equations

Material	Factor Levels	Variable and Measuring Units	Constants* a_1	Constants* a_2
15-5PH	121122	F_R (N; Pounds)	7.1 (1.60)	1.3 (0.29)
15-5PH	222112	F_R (N; Pounds)	15.7 (3.53)	1.2 (0.28)
BeCu	211212	F_R (N; Pounds)	3.9 (0.87)	0.9 (0.21)
BeCu	212121	F_R (N; Pounds)	-8.9 (-2.00)	1.6 (0.36)
BeCu	221221	F_R (N; Pounds)	12.5 (2.80)	-1.6 (-0.35)
Kovar	122211	F_R (N; Pounds)	-12.5 (-2.80)	1.3 (0.29)
Kovar	221221	F_R (N; Pounds)	-3.6 (-0.80)	1.3 (0.29)
Kovar	222112	F_R (N; Pounds)	5.9 (1.33)	0.8 (0.19)
Hiperco	111111	F_R (N; Pounds)	-20.1 (-4.53)	10.0 (2.24)
Hiperco	112222	F_R (N; Pounds)	1.2 (0.27)	4.8 (1.08)
Hiperco	121122	F_R (N; Pounds)	10.7 (2.40)	5.2 (1.18)
Hiperco	122211	F_R (N; Pounds)	-32.6 (-7.33)	3.2 (0.72)
Hiperco	211212	F_R (N; Pounds)	17.2 (3.87)	17.7 (3.97)
Hiperco	212121	F_R (N; Pounds)	29.7 (6.67)	8.7 (1.95)
Hiperco	221221	F_R (N; Pounds)	-12.5 (-2.80)	7.8 (1.75)
Hiperco	222112	F_R (N; Pounds)	0.58 (0.13)	8.9 (2.01)
303Se	111111	Burr Thickness (μm; Inch)	53.3 (0.0021)	18.29 (0.00072)

Table A-23 Continued. Constants for Tool-Wear Equations

Material	Factor Levels	Variable and Measuring Units	Constants* a_1	Constants* a_2
303Se	211212	Burr Thickness (μm;Inch)	142.2 (0.0056)	-5.33 (-0.00021)
303Se	221221	Burr Thickness (μm;Inch)	48.3 (0.0019)	10.41 (0.00041)
Hiperco	121122	Burr Thickness (μm;Inch)	33.0 (0.0013)	-4.06 (-0.00016)
Hiperco	211212	Burr Thickness (μm;Inch)	83.8 (0.0033)	-11.18 (-0.00044)
Hiperco	212121	Burr Thickness (μm;Inch)	86.4 (0.0034)	-8.89 (-0.00035)
303Se	221221	Burr Length (μm;Inch)	20.3 (0.0008)	89.15 (0.00351)
15-5PH	212121	Burr Length (μm;Inch)	2.5 (0.0001)	3.81 (0.00015)
Hiperco	121122	Burr Length (μm;Inch)	33.0 (0.0013)	-4.06 (-0.00016)
Hiperco	211212	Burr Length (μm;Inch)	83.8 (0.0033)	-11.18 (-0.00044)
Hiperco	212121	Burr Length (μm;Inch)	55.9 (0.0022)	-5.59 (-0.00022)
Hiperco	221221	Burr Length (μm;Inch)	53.3 (0.0021)	-2.54 (-0.00010)
303Se	111111	Surface Finish (μm;Microinches)	1.77 (69.87)	-0.13 (-5.19)
303Se	112222	Surface Finish (μm;Microinches)	1.31 (51.47)	-0.08 (-3.01)
303Se	222112	Surface Finish (μm;Microinches)	0.16 (6.20)	0.07 (2.85)
15-5PH	112222	Surface Finish (μm;Microinches)	0.08 (3.00)	0.20 (7.76)
15-5PH	121122	Surface Finish (μm;Microinches)	0.66 (25.93)	-0.04 (-1.66)
15-5PH	211212	Surface Finish (μm;Microinches)	0.12 (4.80)	0.03 (1.29)

Table A-23 Continued. Constants for Tool-Wear Equations

Material	Factor Levels	Variable and Measuring Units	Constants a_1	Constants a_2
BeCu	111111	Surface Finish (μm;Microinches)	0.84 (33.00)	0.03 (1.11)
BeCu	112222	Surface Finish (μm;Microinches)	1.33 (52.40)	0.03 (1.02)
BeCu	222112	Surface Finish (μm;Microinches)	0.26 (10.33)	0.03 (1.30)
Kovar	112222	Surface Finish (μm;Microinches)	1.22 (48.20)	0.03 (1.15)
Kovar	121122	Surface Finish (μm;Microinches)	1.37 (53.93)	0.04 (1.38)
Kovar	221221	Surface Finish (μm;Microinches)	1.13 (44.47)	0.06 (2.39)
Hiperco	121122	Surface Finish (μm;Microinches)	0.29 (11.60)	0.06 (2.20)
Hiperco	212121	Surface Finish (μm;Microinches)	0.26 (10.33)	0.03 (1.25)

*These constants are for use in Equation 17 of this report:

$$Y = a_1 + a_2\left(\frac{L}{5.625}\right),$$

where L is the axial length-of-cut in inches and Y is the dependent variable. For example, the first entry in this table, with F_A expressed in pounds, would be

$$F_A = 18.13 + 0.67\left(\frac{L}{5.625}\right).$$

When the SI Metric system of units is used, with F_A expressed in newtons and L in millimeters, the first entry in this table would be

$$F_A = 80.6 + 2.98\left(\frac{L}{142.9}\right).$$

Table A-24. Effects of Speed, Feedrate, and Tool Sharpness, Using Tool Geometry 3 in Annealed 303Se Stainless Steel

Workpiece Number	Spindle Speed (RPM)	Feedrate (μm/Rev; IPR)	Measurements for Indicated Parameters* Force F_T (N; Pounds)	Force F_A (N; Pounds)	Force F_R (N; Pounds)
97	300	127.0 (0.005)	111 (25)	31 (7)	18 (4)
98	450	127.0 (0.005)	142 (32)	27 (6)	36 (8)
99	150	127.0 (0.005)	120 (27)	22 (5)	13 (3)
100	150	35.6 (0.0014)	27 (6)	9 (2)	18 (4)
101	450	35.6 (0.0014)	53 (12)	22 (5)	4 (1)
102	450	12.7 (0.0005)	89 (20)	22 (5)	18 (4)
103	300	12.7 (0.0005)	89 (20)	22 (5)	13 (3)
104	150	12.7 (0.0005)	44 (10)	9 (2)	9 (2)
105**	300	35.6 (0.0014)	67 (15)	31 (7)	4 (1)
106**	300	35.6 (0.0014)	67 (15)	31 (7)	13 (3)
3	300	35.6 (0.0014)	53 (12)	22 (5)	18 (4)
			Fillet Radius (μm; Mils)	Nose Radius (μm; Mils)	Surface Finish (μm; μIn.)
97	300	127.0 (0.005)	35.6 (1.4)	12.7 (0.5)	2.16 (85)
98	450	127.0 (0.005)	61.0 (2.4)	38.1 (1.5)	3.20 (125)

Table A-24 Continued. Effects of Speed, Feedrate, and Tool Sharpness, Using Tool Geometry 3 in Annealed 303Se Stainless Steel

Workpiece Number	Spindle Speed (RPM)	Feedrate (μm/Rev; IPR)	Measurements for Indicated Parameters*		
			Fillet Radius (μm; Mils)	Nose Radius (μm; Mils)	Surface Finish (μm; μ In.)
99	150	127.0 (0.005)	30.5 (1.2)	0 (0)	2.67 (105)
100	150	35.6 (0.0014)	127.0 (5.0)	101.6 (4.0)	0.41 (16)
101	450	35.6 (0.0014)	20.3 (0.8)	25.4 (1.0)	1.14 (45)
102	450	12.7 (0.0005)	45.7 (1.8)	25.4 (1.0)	2.72 (107)
103	300	12.7 (0.0005)	17.8 (0.7)	38.1 (1.5)	2.08 (82)
104	150	12.7 (0.0005)	53.3 (2.1)	76.2 (3.0)	1.45 (57)
105**	300	35.6 (0.0014)	101.6 (4.0)	50.8 (2.0)	1.12 (44)
106**	300	35.6 (0.0014)	101.6 (4.0)	63.5 (2.5)	0.74 (29)
3	300	35.6 (0.0014)	35.6 (1.4)	***	1.47 (58)
			Burr Height (μm; Mils)	Burr Thickness (μm; Mils)	
97	300	127.0 (0.005)	63.5 (2.5)	58.4 (2.3)	
98	450	127.0 (0.005)	83.8 (3.3)	33.0 (1.3)	
99	150	127.0 (0.005)	124.5 (4.9)	127.0 (5.0)	
100	150	35.6 (0.0014)	127.0 (5.6)	104.1 (4.1)	

Table A-24 Continued. Effects of Speed, Feedrate, and Tool Sharpness, Using Tool Geometry 3 in Annealed 303Se Stainless Steel

Workpiece Number	Spindle Speed (RPM)	Feedrate (μm/Rev; IPR)	Measurements for Indicated Parameters* Burr Height (μm; Mils)	Burr Thickness (μm; Mils)	
101	450	35.6 (0.0014)	101.6 (4.0)	88.9 (3.5)	
102	450	12.7 (0.0005)	99.1 (3.9)	96.5 (3.8)	
103	300	12.7 (0.0005)	160.0 (6.3)	16.0 (4.6)	
104	150	12.7 (0.0005)	83.8 (3.3)	104.1 (4.1)	
105**	300	35.6 (0.0014)	401.3 (15.8)	561.3 (22.1)	
106**	300	35.6 (0.0014)	320.0 (12.6)	114.3 (4.5)	
3	300	35.6 (0.0014)	243.8 (9.6)	96.5 (3.8)	
			Wearland A**** (μm; Mils)	Wearland B (μm; Mils)	Wearland C (μm; Mils)
97	300	127.0 (0.005)	0 (0)	0 (0)	0 (0)
98	450	127.0 (0.005)	203.2 (8.0)	50.8 (2.0)	0 (0)
99	150	127.0 (0.005)	0 (0)	0 (0)	0 (0)
100	150	35.6 (0.0014)	508.0 (20.0)	76.2 (3.0)	25.4 (1.0)
101	450	35.6 (0.0014)	114.3 (4.5)	50.8 (2.0)	50.8 (2.0)
102	450	12.7 (0.0005)	139.7 (5.5)	68.6 (2.7)	0 (0)

Table A-24 Continued. Effects of Speed, Feedrate, and Tool Sharpness, Using Tool Geometry 3 in Annealed 303Se Stainless Steel

Workpiece Number	Spindle Speed (RPM)	Feedrate (μm/Rev; IPR)	Measurements for Indicated Parameters* Wearland A**** (μm; Mils)	Wearland B (μm; Mils)	Wearland C (μm; Mils)
103	300	12.7 (0.0005)	50.8 (2.0)	50.8 (2.0)	0 (0)
104	150	12.7 (0.0005)	228.6 (9.0)	88.9 (3.5)	38.1 (1.5)
105**	300	35.6 (0.0014)	114.3 (4.5)	50.8 (2.0)	30.5 (1.2)
106**	300	35.6 (0.0014)	533.0 (21.0)	139.7 (5.5)	63.5 (2.5)
3	300	35.6 (0.0014)	***		

*Values shown are the average of two readings, with the exception of cutting-tool nose radius and wearland size.
**Samples 105 and 106 were produced with dull tools.
***Blank space indicates that no measurement was made.
****Refer to Figure 22 for definition of wearland positions.

DISTRIBUTION

	Copy
R. Bulcock, ERDA-KCAO, 1D49	1
J. E. Green, G. E. Pinellas	2
J. W. Baker, Rocky Flats	3
K. Thistlewood, Rocky Flats	4
G. P. Ford, SLA	5
K. Gillespie, SLA	6
R. S. Pinkham, SLA	7
A. L. Thornton, SLA	8
W. Johaningsmeir, D/231, 1D40	9
H. L. Price, D/261, FU34	10
E. L. Young, D/261, FU34	11
B. H. Neal, D/411, 2E29	12
H. T. Barnes, D/554, BD50	13
J. D. Corey, D/554, BD50	14-15
L. Stratton, D/554, 2C44	16-18
E. F. Felkner, D/752, 1A41	19
J. D. Johnson, D/752, 1A41	20
R. F. Cell, D/755, 1A42	21
R. P. Frohmberg, D/800, 2A39	22
J. A. Knuth, D/800/D. D. Oswald/J. P. Dycus/ D. R. Wachter, D/822, 1A44	23
J. L. Couchman/F. J. Boyle/B. W. Landes, D/821, 2A36	24
R. K. Albright, D/822, 2A36	25
G. R. Flebbe, D/822, 2A36	26
L. K. Gillespie, D/822, 2A36	27-43
G. E. Klement, D/822, 2A36	44
W. P. McKay, D/822, 2A36	45
J. M. Robb, D/822, 2A36	46
D. P. Roberts/C. E. Spitzkeit, D/823, 2A36	47
R. W. Lange, D/861, 2A31	48
R. E. Kessler, D/865, 2C40	49

BDX-613-1723

MACHINABILITY OF METALS AS RELATED TO MINIATURE PRECISION COMPONENTS, L. K. Gillespie, D/822, UNCLAS Topical, January 1978.

A study to determine how tool geometry and workpiece material can be selected to produce low cutting forces, small fillet radii, smooth surface finishes, and burr-free edges required for the production of reliable miniature precision parts has indicated that tool geometries typically specified for general machining applications produce optimum results. Surface finishes of 0.56 to 1.07 μm

MECHANICAL: Precision-Turned Parts

MACHINABILITY OF METALS AS RELATED TO MINIATURE PRECISION COMPONENTS, L. K. Gillespie, D/822, UNCLAS Topical, BDX-613-1723, January 1978.

A study to determine how tool geometry and workpiece material can be selected to produce low cutting forces, small fillet radii, smooth surface finishes, and burr-free edges required for the production of reliable miniature precision parts has indicated that tool geometries typically specified for general machining applications produce optimum results. Surface finishes of 0.56 to 1.07 μm

MACHINABILITY OF METALS AS RELATED TO MINIATURE PRECISION COMPONENTS, L. K. Gillespie, D/822, UNCLAS Topical, BDX-613-1723, January 1978.

A study to determine how tool geometry and workpiece material can be selected to produce low cutting forces, small fillet radii, smooth surface finishes, and burr-free edges required for the production of reliable miniature precision parts has indicated that tool geometries typically specified for general machining applications produce optimum results. Surface finishes of 0.56 to 1.07 μm

AA (22 to 40 microinches) can be produced while maintaining 76.2-μm (0.003 inch) fillet radii in ferrous and beryllium-copper alloys. Tool life is extremely short when fillet radii less than 76.2 μm must be maintained. Materials having high strain-hardening exponents produce large burrs.

AA (22 to 40 microinches) can be produced while maintaining 76.2-μm (0.003 inch) fillet radii in ferrous and beryllium-copper alloys. Tool life is extremely short when fillet radii less than 76.2 μm must be maintained. Materials having high strain-hardening exponents produce large burrs.

AA (22 to 40 microinches) can be produced while maintaining 76.2-μm (0.003 inch) fillet radii in ferrous and beryllium-copper alloys. Tool life is extremely short when fillet radii less than 76.2 μm must be maintained. Materials having high strain-hardening exponents produce large burrs.